GeroScience (2022) 44:2105–2128
https://doi.org/10.1007/s11357-022-00529-z

ORIGINAL ARTICLE

Immune phenotype of the CD4$^+$ T cells in the aged lymphoid organs and lacrimal glands

Claudia M. Trujillo-Vargas · Kelsey E. Mauk · Humberto Hernandez · Rodrigo G. de Souza · Zhiyuan Yu · Jeremias G. Galletti · Jana Dietrich · Friedrich Paulsen · Cintia S. de Paiva

Received: 21 October 2021 / Accepted: 11 February 2022 / Published online: 12 March 2022

Abstract Aging is associated with a massive infiltration of T lymphocytes in the lacrimal gland. Here, we aimed to characterize the immune phenotype of aged CD4$^+$ T cells in this tissue as compared with lymphoid organs. To perform this, we sorted regulatory T cells (Tregs, CD4$^+$CD25$^+$GITR$^+$) and non-Tregs (CD4$^+$CD25^{neg}GITR^{neg}) in lymphoid organs from female C57BL/6J mice and subjected these cells to an immunology NanoString® panel. These results were confirmed by flow cytometry, live imaging, and tissue immunostaining in the lacrimal gland. Importantly, effector T helper 1 (Th1) genes were highly upregulated on aged Tregs, including the master regulator *Tbx21*. Among the non-Tregs, we also found a significant increase in the levels of EOMES$^{med/high}$, Tbet^{neg}IFN-γ$^+$, and CD62L$^+$CD44^{neg}CD4$^+$ T cells with aging, which are associated with cell exhaustion, immunopathology, and the generation of tertiary lymphoid tissue. At the functional level, aged Tregs from lymphoid organs are less able to decrease proliferation and IFN-γ production of T responders at any age. More importantly, human lacrimal glands

Supplementary Information The online version contains supplementary material available at https://doi.org/10.1007/s11357-022-00529-z.

C. M. Trujillo-Vargas
Grupo de Inmunodeficiencias Primarias, Facultad de Medicina, Universidad de Antioquia, UdeA, Medellín, Colombia
e-mail: claudia.trujillo@udea.edu.co

C. M. Trujillo-Vargas · H. Hernandez · R. G. de Souza · Z. Yu · C. S. de Paiva (✉)
Department of Ophthalmology, Ocular Surface Center, Cullen Eye Institute, Baylor College of Medicine, 6565 Fannin Street, Houston, TX NC 505G, USA
e-mail: cintiadp@bcm.edu

R. G. de Souza
e-mail: rodrigoguimaraes.rgs@gmail.com

Z. Yu
e-mail: zhiyuan.yu@bcm.edu

K. E. Mauk
Graduate Program in Immunology & Microbiology, Baylor College of Medicine, Houston, TX, USA
e-mail: Kelsey.mauk@bcm.edu

J. G. Galletti
Institute of Experimental Medicine, CONICET-National Academy of Medicine of Buenos Aires, Buenos Aires, Argentina
e-mail: jeremiasg@gmx.net

J. Dietrich · F. Paulsen
Institute of Functional and Clinical Anatomy, Friedrich-Alexander-Universität Erlangen-Nürnberg, Erlangen, Germany
e-mail: jana1.dietrich@fau.de

F. Paulsen
e-mail: friedrich.paulsen@fau.de

(age range 55–81 years) also showed the presence of $CD4^+Foxp3^+$ cells. Further studies are needed to propose potential molecular targets to avoid immune-mediated lacrimal gland dysfunction with aging.

Keywords Aging · Lymphoid organs · Lacrimal gland · Dry eye disease · Sjögren's syndrome · $CD4^+$ T cells · Regulatory T cells · Conventional T cells · Transcriptome

Introduction

Over the last century, aging has become a topic of the utmost importance for humans due to the accelerated increase in life expectancy. Thus, elucidation of new biological mechanisms for cell renewal, rejuvenation, and improving quality of life in the elderly is the modern alchemy in science.

Aging changes are not unfamiliar for the immune system; evidence has demonstrated structural alterations in lymphoid organs, redistribution in the different cell subpopulation, and adjustments in the primary and secondary responses to antigens [1, 2]. Overall, this process is called immunosenescence. One of the most intriguing events of immunosenescence is the lymphocyte invasion to non-lymphoid tissues with chronic inflammation and the formation of tertiary lymphoid tissue (TLT) [3–5]. At the ocular surface, aging has been associated with an increased prevalence of keratoconjunctivitis sicca (KCS), also called dry eye disease, especially in women [6]. Interestingly, this condition is more frequent in patients with autoimmune conditions such as Sjögren's syndrome (SS), systemic lupus erythematosus, rheumatoid arthritis, and diabetes mellitus, among others [6]. As early as 1973, Williamson et al. [7] described that KCS and SS were highly associated with infiltration of lymphocytes, acinar atrophy, and fibrosis of the lacrimal gland [7]. Several groups including ours have studied lymphocyte infiltration of the lacrimal gland in the aged mice [8–10]. One of the most remarkable inquiries in the process of lymphocyte invasion during aging is the phenotypic signature and role of $CD4^+$ T cells as helper players, in the recruitment of the other subpopulations of immune cells throughout the tissues. During the process of TLT formation in the thyroid, it is known that the development of dendritic cell–activated mature $CD4^+$ T cells, together with the formation of highly differentiated high endothelial venules, rather than the presence of $CD3^{neg}CD4^+$ lymphoid tissue inducer cells, recreates a chemokine environment suitable for the attraction and organization of other immune cells [11]. Together with the change in the phenotype and function of conventional $CD4^+$ T cells, $CD4^+Foxp3^+$ regulatory T cells (Tregs) mobilize and infiltrate the tissues with aging, especially in lymphoid organs [12, 13]. Tregs in elderly spleen exhibit an activated phenotype with increased expression of CD103, CD69, interleukin (IL)-10, and PD-1; hypomethylation of the Foxp3 enhancer; differential usage of some V beta genes; and decreased susceptibility to apoptosis [13–15].

Despite all the information about T conventional and Treg interplay in the lymphoid organs in elderly mice, scarce findings exist in human tissues. Most of the studies are focused on the phenotyping of circulating T cell subpopulations [13, 16]. Interestingly, Derhovanessian et al. [17] found that increased circulating $CCR4^+$ Tregs were correlated with better 8-year survival in elderly individuals. In human salivary gland biopsies, the frequency of $Foxp3^+$ cells correlates with the systemic severity score in SS patients [18, 19].

We have investigated the connection between lacrimal gland lymphocyte infiltration and autoimmune-like changes in aged mice. By using the non-obese diabetic mouse model, which has great similarity to the SS in humans, we demonstrated that the lacrimal glands of these animals have augmented infiltration of Tregs with aging and these Tregs have adopted for the expression of IFN-γ or IL-17 [20], which has been shown to improve their suppressive capabilities against the conventional T cells in the tissue microenvironment [21]. The same was observed in aged C57BL/6J mice with accumulation of conventional T helper 1 (Th1) cells [22].

Here, we further characterize the phenotype of Tregs and non-Tregs in the aged murine lacrimal gland as compared to the lymphoid organs. We used a combination of cell sorting and NanoString® technology to define the immune-related differentially expressed genes (DEGs) in both subpopulations in mixtures of eye-draining cervical lymph nodes (CLNs) and spleens of young and aged mice. Based on these findings, we investigated the Treg and non-Treg phenotype in the lacrimal gland with flow cytometry and live imaging. The function of Tregs

from lymphoid organs was evaluated by using the Treg suppression assay. More importantly, we characterized the lymphocyte immunophenotype in several human lacrimal glands by using immunofluorescence. Our results indicate that aged murine Tregs share features of activated memory effector cells. However, the Treg immune–related transcriptome arsenal seems insufficient to regulate the exhausted non-Tregs. These results were confirmed in lymphoid organs by the Treg suppression assay. More importantly, aged murine lacrimal glands also exhibited greater percentages of naïve T cells as compared to their young counterparts. We also detected $CD4^+Foxp3^+$ cells in aged human lacrimal glands. The molecular characterization of the immune landscape in the lacrimal gland will provide novel molecular targets either to delay the aging process or, better, to rejuvenate the ocular surface.

Results

T regulatory cells are increased in the lacrimal glands and lymphoid organs of aged mice

Our group has demonstrated an increase in the numbers of Tregs in the lacrimal gland of aged non-obese diabetic mice [20]. In patients with SS, increased $Foxp3^+$ cell infiltration in minor salivary gland biopsies correlates with increased systemic severity [18, 19]. Therefore, we investigated the levels of $CD4^+Foxp3^+$ T regulatory lymphocytes (Tregs) in cell suspensions of the lacrimal gland, draining CLN and spleens from young and aged C57BL/6J mice by flow cytometry. We found a significant increase in the percentage of Tregs in these tissues with aging (Fig. 1A). In inflammatory conditions, it has been shown that Tregs downregulate its Foxp3 expression, becoming "ex-Foxp3" and, potentially, inflammatory cells [23]. In this study, the Foxp3 mean fluorescence intensity (MFI) did not vary among age groups (Fig. 1B).

We then aimed to characterize the transcriptome of these cells from both groups of mice using a NanoString® Immunology Panel. Because of the difficulty to use the intracellular marker Foxp3 for sorting of living Tregs, we evaluated the expression of the glucocorticoid-induced TNFR-related (GITR) protein as a potential extracellular surrogate marker for Foxp3. GITR is highly expressed in Tregs [24] and either equally expressed or slightly increased in young as compared to aged splenocytes in mice [13, 25]. We obtained similar results in our experiments, in which we only found a slight decrease in the GITR MFI in the surface of aged Tregs in mouse lymphoid tissues (Fig. 1C). Therefore, we used this strategy in

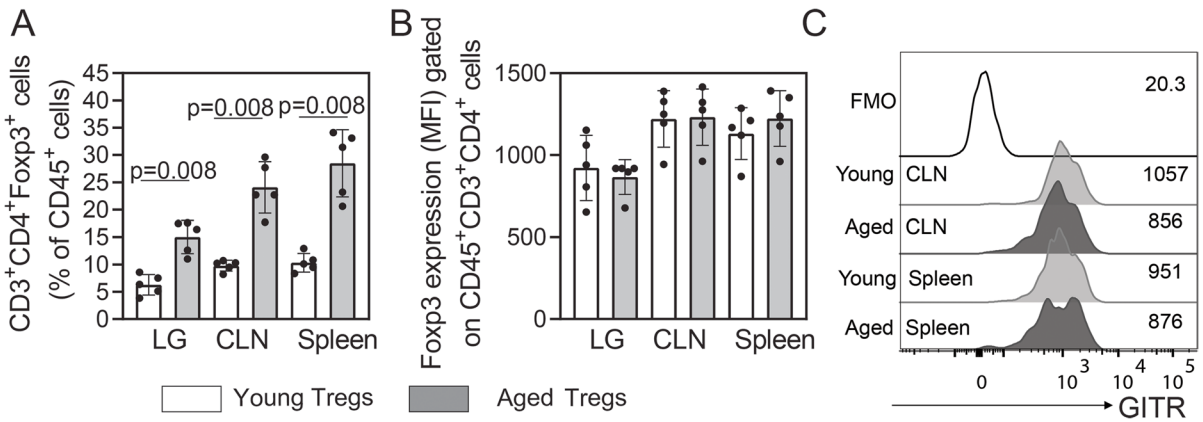

Fig. 1 $CD4^+$ $Foxp3^+$ T cells accumulate in aged lacrimal gland as well as in lymphoid tissues. Single cell suspensions were obtained from the lacrimal gland (LG), ocular, and LG draining cervical lymph nodes (CLNs) and spleen of young and aged mice ($n=5$ per group), to quantify **A** the percentages and **B** median fluorescence intensity (MFI) of alive $CD45^+CD3^+CD4^+$ cells expressing Foxp3 intracellularly (Tregs). **C** The extracellular expression of GITR was also evaluated in Tregs from CLN and spleen cell suspensions by flow cytometry. Numbers at the right side of the histogram indicate the MFI of GITR. Values in the bars expressed as mean ± standard deviation. Statistical significance based on Mann–Whitney *U* test. The significant *p* value is indicated above the bars

the sorting of Tregs ($CD4^+CD25^+GITR^+$) and compared them to non-Tregs ($CD4^+CD25^{neg}GITR^{neg}$). To do this, we pooled a mixture of CLN and spleen cell suspensions from three mice as one sample from young and aged mice and examined their transcriptome. We obtained a total of 5–7 biological replicates per age group. Supplementary Fig. 1 shows a representative example of the sorting strategy.

Highly activated effector memory Tregs are found in the lacrimal glands and lymphoid organs from aged mice

An overall look at the transcriptional expression of the 547 genes from the mouse immunology NanoString® panel suggested that 128 DEGs were upregulated in aged Tregs as compared to their young counterparts and only 43 genes were downregulated (Fig. 2A and Supplementary Table 1). Supplementary Fig. 2 classified all the genes from the NanoString® Immunology panel according to their nSolver® immunology descriptors, specifying if they are upregulated, downregulated, or unaffected in aged as compared to young Tregs. Most of the upregulated genes were classified as associated with lymphocyte activation, host–pathogen interaction, and cytokine signaling, although some genes were assigned to more than one pathway in the panel (Supplementary Fig. 1).

The most significantly modulated transcripts encode molecules involved in activation (H2-related genes, *Sell*, *Ccr7*, and *IL6ra*), Th1 responses (*Tbx21*, encoding Tbet; *Cxcl10*), or suppressive activity (*Cd81*) (Fig. 2B). The expression of the Treg markers was equally expressed in young and aged Tregs, including *Foxp3*, *Ctla4*, *Il10*, and *Tgfb*. *Icos* was upregulated in Tregs from lymphoid tissues in aged mice (Fig. 2C), which agrees with previously published evidence [26]. The same pattern was observed for *Pdcd1* encoding the programmed cell death protein 1 (PD-1), an important immune checkpoint inhibitor. Among the transcripts related to Treg activation, MHC-related genes such as *H2-Eb1*, *H2-Ab1*, *H2-Aa*, *Cd74*, *H2-DMb2*, *H2-Q10*, and *H2-DMa* were significantly upregulated in aged Tregs. MHC expression in Tregs increases immune suppression [27]; however, the impact of the different MHC haplotypes on the function of these cells has not been investigated. *Tnfsf13b* encodes the cytokine B cell activation factor of the TNF family, BAFF, a co-stimulatory receptor for B cell–mediated responses. BAFF transgenic mice have expanded $CD25^+Foxp3^+$ Tregs with a cell surface phenotype consistent with an increased activation status and enhanced ability to home to inflamed sites [28]. *Ccr2*, *Cd81*, and *Tnfrsf4* are involved in the trafficking of Tregs to tumors [29, 30]. *Il1r2*, encoding a decoy receptor for IL-1, was highly expressed in activated aged Tregs. *Pdgfb*, *Gzmb*, *Maf*, *Batf*, *Ccr2*, *Ahr*, *Ccrl2*, *Il1rl1*, *Icos*, *Icam1*, and *Tnfrsf4* are genes involved in the control of inflammation by effector Tregs in different tissues [31–36]. We also observed loss of the transcripts for CD62 ligand (CD62L, encoded by *Sell*), *Ccr7*, *Lef1*, and *Cd7*.

Figure 2D shows the normalized counts for two of the activation-related genes upregulated in the aged Tregs: *Il1r2* and *CD81*, whose expression was validated by flow cytometry in the lacrimal glands, CLN, and spleen of young and aged animals. The three tissues upregulated these markers in Tregs at the protein level, an effect that was more pronounced in the spleen (Fig. 2E). We also selected another characteristic activation marker, the adhesion molecule CD44 for the flow cytometry analysis, as $CD44^+$ Tregs are more potent in suppressing effector T cell proliferation [37]. The expression of this molecule was also augmented in aged as compared with young Tregs in the three tissues evaluated (Fig. 2F).

This Treg signature is compatible with a highly activated, effector memory phenotype and shortened telomeres in chronic inflammatory lesions [38].

Aged Tregs highly expressed the transcript for the master regulator of T helper 1 responses, Tbet, and other related genes in the lymphoid tissues and lacrimal gland

A common immune-mediated disorder of the ocular surface, especially in the elderly, is dry eye disease [6]. This condition is mediated by cytokine-producing Th1 and Th17 effector cells that cause ocular surface inflammation and epithelial disease [39–41]. Our research has discovered increased numbers of T regs in autoimmune mice, with rather impaired suppressive function, and accompanying age-related inflammation in the lacrimal gland [20].

Next, we classified and characterized the DEGs related to effector Th cell responses in the two groups of Tregs from the lymphoid tissue. It has been demonstrated that Tregs utilize the transcription

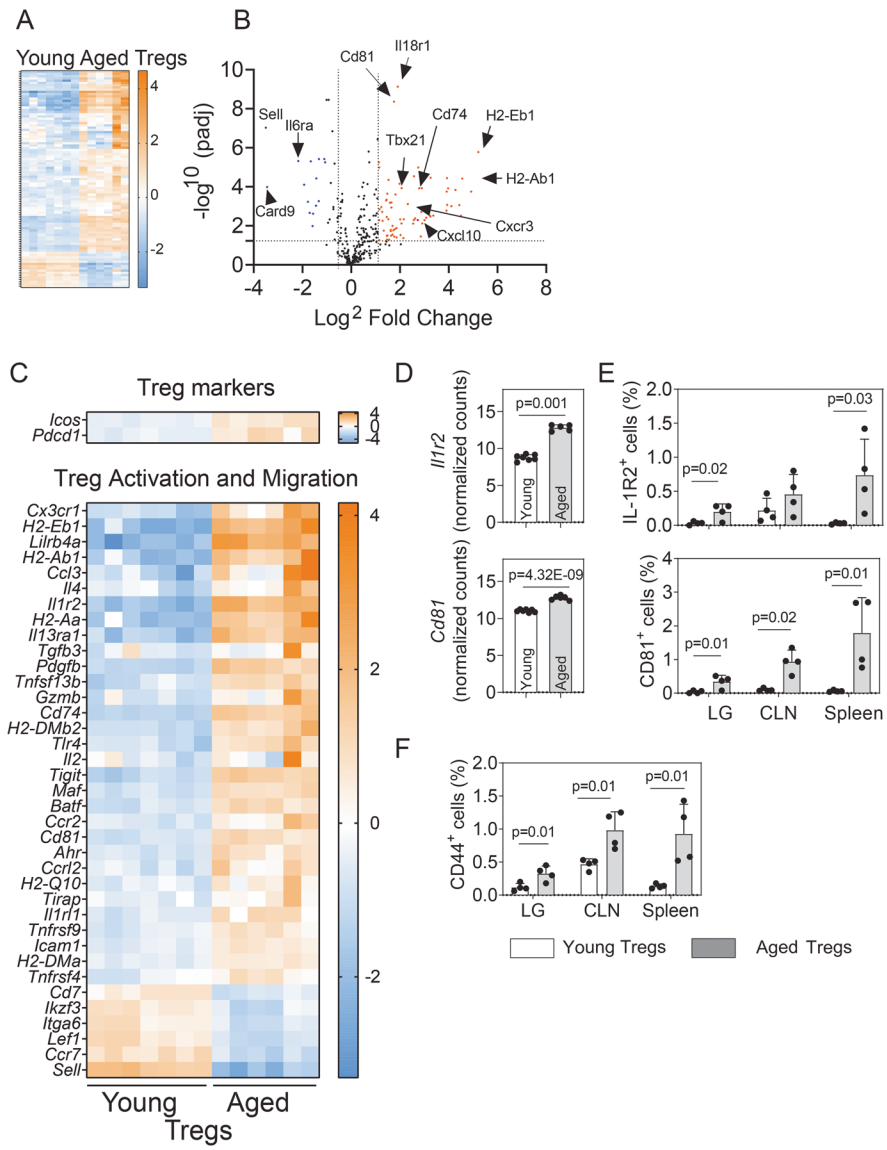

Fig. 2 Comparative analysis of expressed immune-related genes in aged versus young Tregs. RNA from sorted cells ($n=5$–7 biological replicates/group; each replicate include the CLN and spleens from three mice) was isolated and subjected to NanoString® analysis. **A** The overall gene expression profile for the 547 molecular targets included in the panel is shown. **B** The volcano plot shows the magnitude of change of the lymphoid organ genes modulated by aging (log2 fold change) versus the adjusted p value ($-\log10$). Some of the most significantly upregulated and downregulated genes are highlighted. The dotted line indicates a significance of 0.05. **C** Detailed analysis of significantly differentially expressed genes (DEGs) greater than twofold change associated with Treg function and activation. **D** Normalized counts of two upregulated DEGs (*Il1r2*, *Cd81*) from NanoString® analysis. p value indicates FDR from ROSALIND® software, calculated as described in the "Methods." **E**, **F** Flow cytometry analysis of protein expression of Il1r2 and CD81 **E** and CD44 **F** in the lacrimal gland (LG), draining cervical lymph nodes (CLNs) and spleen in young (2–3 months) and aged (22–25 months) mice ($n=4$ mice per group). Values in the bars expressed as mean ± standard deviation. Statistical significance based on the Mann–Whitney U test. The significant p value is indicated above the bars

factor program of the population they are suppressing [42], which allows them to control the effector T cell population and adapt to environmental cues. In our NanoString® analysis, many transcripts

related to Th1-Tregs were differentially expressed; Fig. 3A depicts them in a numerical order of the differential expression. *Tbx21* was highly upregulated in aged lymphoid tissues (Fig. 3A). Interestingly, *Il12rb2* was not differentially expressed with aging, suggesting that these cells might be unresponsive to IL-12 ex vivo as it has been previously reported [43].

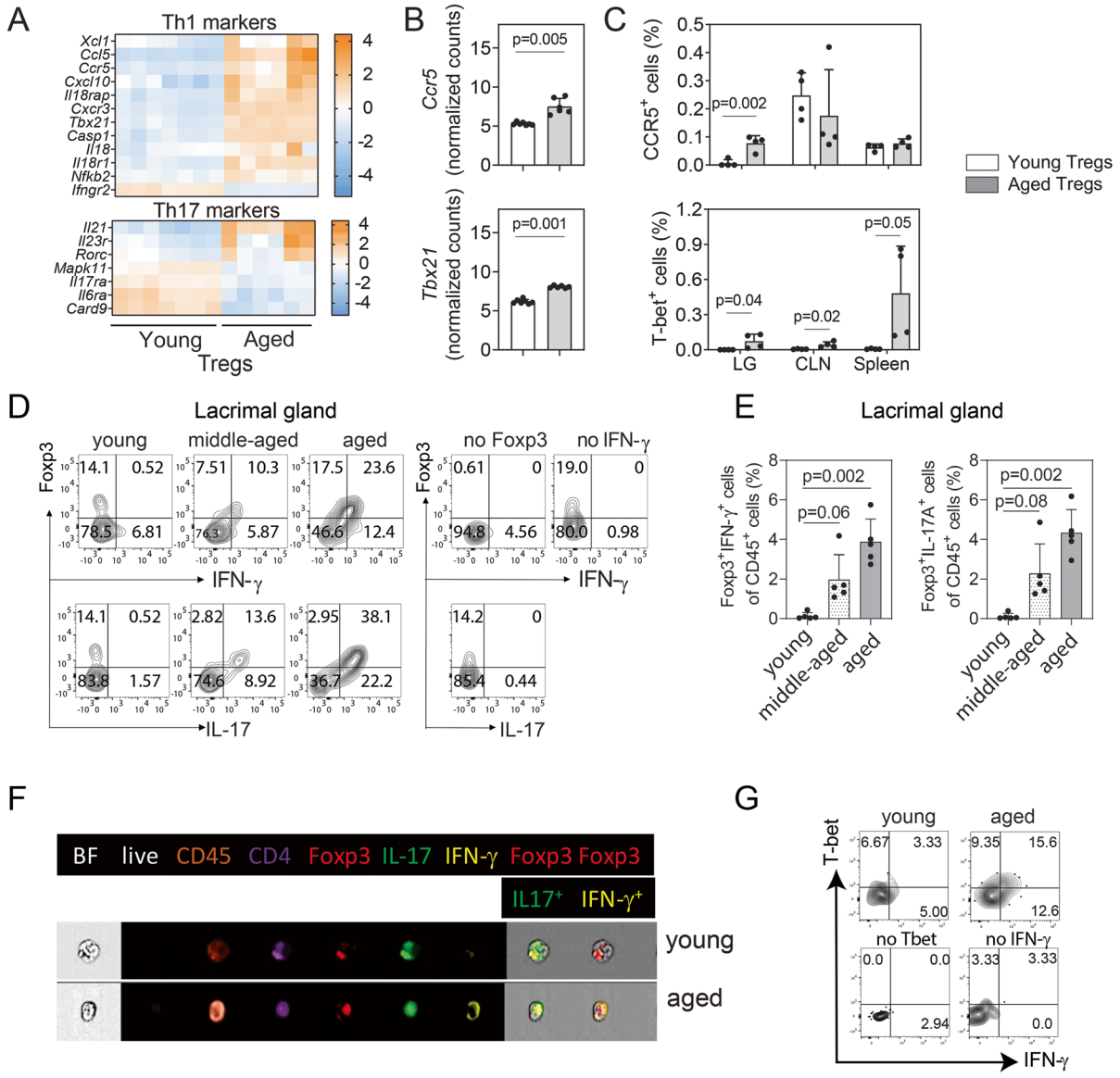

Fig. 3 Effector Tregs accumulate in the aged lacrimal glands as compared with lymphoid tissues. **A** Heatmap of the expression of Th1- and Th17-related genes was compared in young and aged lymphoid tissues. **B** Normalized counts of *Ccr5* and *Tbx21* in the analyzed samples together with **C** the flow cytometry analysis of the corresponding protein expression in the lacrimal gland (LG), draining cervical lymph node (CLN) and spleen ($n=4$ animals per group). **D** Representative contour plots of cytokine-producing $CD4^+Foxp3^+$ lymphocytes in the lacrimal gland in mice at different time points by flow cytometry. **E** Cumulative data of all the samples analyzed ($n=5$ animals per group). **F** The same parameters by live imaging are also shown ($n=3$ animals per group). **G** Representative contour plots of the co-expression of Tbet and IFN-γ by flow cytometry in young and aged lacrimal glands ($n=4$ animals per group). Values in the bars expressed as mean ± standard deviation. Statistical significance based on the Mann–Whitney *U* test. The significant *p* value is indicated above the bars

Similar heatmaps for the Th17-related markers are presented in Fig. 3A. Few Th17-associated genes were upregulated with aging (*Il21*, *Il23r*, *Rorc*). Next, we singled out the normalized counts for two of the Th1-associated upregulated genes in aged lymphoid tissues, *Ccr5* and *Tbx21*, in young and aged Tregs (Fig. 3B). The upregulation of these molecules, at the protein level, was also investigated by flow cytometry in young and aged Tregs from lacrimal glands, CLN, and spleen (Fig. 3C). Interestingly, we did not observe an increase in the protein expression of CCR5 in aged lymphoid organ Tregs, although it was significantly upregulated in aged Tregs from the lacrimal glands. Intracellular Tbet expression was significantly upregulated in all tissues, especially in the spleen.

We also evaluated if Foxp3 and either IFN-γ or IL-17A were co-expressed in $CD4^+$ cells from the aged lacrimal gland as compared with young and middle-aged mice (Fig. 3D). In young mice, we observed the presence of $CD4^+Foxp3^+$ cells in the murine lacrimal glands; however, the great majority of them were either IFN-γ or IL-17A negative. This expression pattern shifted as early as middle age (12–13 months of age in mice), when we observed that 60–80% of the $CD4^+Foxp3^+$ cells were also expressing IFN-γ or IL-17A intracellularly. These subpopulations of cells notoriously increased in the aged murine lacrimal glands. Figure 3E also shows the increase in percentages of the $CD4^+Foxp3^+IFN\text{-}\gamma^+$ and $CD4^+Foxp3^+IL\text{-}17A^+$ cells in the lacrimal gland, normalized to total $CD45^+$ cells. These cytokine-producing $CD4^+Foxp3^+$ cells that were hardly detected in young lacrimal glands represent about 2% of the leukocytes in middle-aged mice and duplicate in the aged mice. The presence of these $CD4^+Foxp3^+IFN\text{-}\gamma^+$ and $CD4^+Foxp3^+IL\text{-}17A^+$ cells was also confirmed by live imaging cytometry comparing young and aged lacrimal glands (Fig. 3F).

Our next experimental approach investigated if the aged lacrimal gland $IFN\text{-}\gamma^+$ Tregs concomitantly expressed Tbet, since $T\text{-}bet^+$ Treg cells do not typically produce IFN-γ [44]. Our analysis demonstrated that most of the Tregs infiltrating the aged lacrimal gland express simultaneously Tbet and IFN-γ (Fig. 3G). Interestingly, $IFN\text{-}\gamma^+Tbet^+$ Tregs have been associated to infection-induced immunopathology [45, 46]. These results confirmed that the Tregs in the lacrimal gland are enriched in Th1-Tregs that concomitantly expressed Tbet and IFN-γ.

Aged T conventional cells are highly exhausted and associated to immunopathology

Previous work has demonstrated remarkable changes in the microarchitecture of the spleen and lymph nodes with age, with disorganized compartmentalization and altered density of different cell subpopulations, which may impact the mucosal immune responses [47]. Interestingly, the age-related changes in the T cells are more prominent in $CD8^+$ T cells than in $CD4^+$ T cells [48]. However, there is still incomplete information about the singularities of the $CD4^+$ T cell immunophenotype in the lymphoid organs and lacrimal gland with aging and the triggers that induce their distinctive reorganization, migration, and activation. Therefore, we also aimed to characterize the immune-related transcriptome of the conventional $CD4^+$ T cells (non-Tregs, $CD4^+CD25^{neg}GITR^{neg}$) in the CLN + spleen suspensions of young and aged C57BL/6 J mice and investigate if the phenotype is recapitulated in the lacrimal gland. There were many DEGs in the aged $CD4^+$ non-Tregs from lymphoid organ genes, compared to young counterparts (volcano plot in Fig. 4A and Supplementary Table 2). In elderly lymphoid organs, we found that the conventional $CD4^+$ T cell transcriptome mainly consisted of DEGs related to activation, effector memory, and susceptibility to apoptosis such as *Cybb*, *Csf1*, *Ccr2*, *Nfil3*, *Ccrl2*, *Tnfrsf4*, and *Casp3*. This also correlated with the decreased expression of the chemokine receptor *Ccr7* and the membrane complement inhibitor *Cd55* (Fig. 4B). The most highly expressed gene in the $CD4^+$ compartment of aged lymphoid organs, *Ccl3*, is associated with the active recruitment of $CD8^+$ T cells [49], one of the hallmarks of the aging [50]. In our analysis, *Entpd1* and *Tnfrsf11*, encoding CD39 and the TNF family cytokine RANKL, respectively, were also significantly upregulated in aged $CD4^+$ non-Tregs. Other upregulated transcripts, such as *Cd80, Ccr6, and Cd74 , have been associated with lymphocyte tissue infiltration [51–53] (Fig. 4B).*

Aging has been associated with the predominance of inhibitory receptors in memory T cells which make them hyporesponsive [54]. Among the inhibitory markers, the most highly upregulated transcript in aged non-Tregs was *IL1r2*. Transcripts for *Il10*, *Pdcd1*, *Ctla4*, and *Icos* were greatly upregulated in aged $CD4^+$ non-Tregs (Fig. 4B). Of note, among the inhibitory genes upregulated in aged $CD4^+$ T cells,

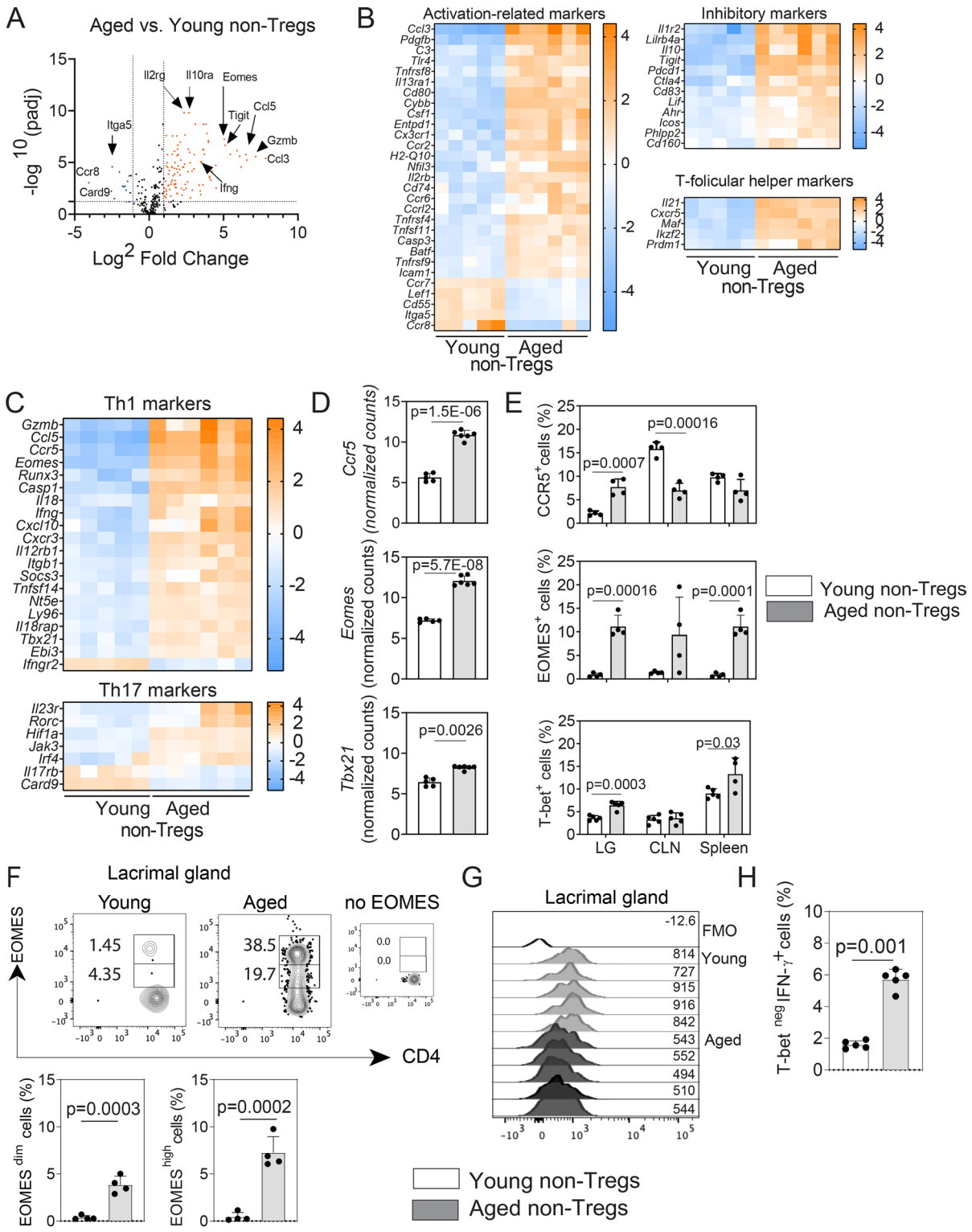
A
Aged vs. Young non-Tregs
-log 10 (padj)
Log2 Fold Change
Il2rg
Il10ra
Eomes
Ccl5
Tigit
Itga5
Gzmb
Ccl3
Ccr8
Card9
Ifng
B
Activation-related markers
Inhibitory markers
T-folicular helper markers
Young
Aged
non-Tregs
C
Th1 markers
Th17 markers
D
Ccr5 (normalized counts)
Eomes (normalized counts)
Tbx21 (normalized counts)
p=1.5E-06
p=5.7E-08
p=0.0026
E
CCR5+ cells (%)
EOMES+ cells (%)
T-bet+ cells (%)
p=0.0007
p=0.00016
p=0.0001
p=0.0003
p=0.03
LG
CLN
Spleen
Young non-Tregs
Aged non-Tregs
F
Lacrimal gland
Young
Aged
no EOMES
EOMES
CD4
1.45
4.35
38.5
19.7
EOMES dim cells (%)
EOMES high cells (%)
p=0.0003
p=0.0002
G
Lacrimal gland
FMO
Young
Aged
H
T-bet neg IFN-γ+ cells (%)
p=0.001

◂**Fig. 4** Aged non-Tregs exhibited an aberrant phenotype associated with activation, exhaustion, and signs of immunopathology. RNA from sorted non-Tregs ($n = 5$–7 biological replicates/group; each replicate includes the CLN and spleens from three mice) was isolated from the lymphoid organs of young and aged mice and subjected to NanoString® analysis. **A** Volcano plot denotes the distribution of the expressed genes according to the significance and the fold change expression, as compared to young and aged Tregs. Some of the most significant upregulated and downregulated genes are highlighted. The dotted line indicates a significance of 0.05. **B**, **C** Heatmaps of the differentially expressed genes (DEGs) associated with activation, inhibition, T follicular help and Th1/Th17 differentiation, and function. **D** Bar graphs depicting the normalized counts of *Ccr5*, *Eomes* , and *Tbx21* DEGs. *p* value indicates FDR from ROSALIND® software, calculated as described in the "Methods." **E** Flow cytometry analysis of the corresponding protein expression in the lacrimal gland (LG), draining cervical lymph node (CLN) and spleen ($n = 4$ animals/group). **F** Histograms showing the EOMES expression pattern in young and aged non-Tregs in the lacrimal glands together with the flow cytometry analysis of the $EOMES^{dim}$ and $EOMES^{high}$ cells in the lacrimal gland by flow cytometry. **G** Histogram showing the expression of Tbet in non-Tregs. **H** Flow cytometry analysis showing $Tbet^{neg}$/IFN-γ^+ cells ($n = 5$ animals/group). Values in the bars expressed as mean ± standard deviation. Statistical significance based on the Mann–Whitney *U* test. The significant *p* value is indicated above the bars

Ahr has been shown to modulate effector T cell function [55].

Follicular helper T (T_{fh}) cells, characterized by the expression of the chemokine receptor CXCR5, IL-21, and the transcription factor BCL-6, are essential to provide B cell help in the germinal centers. We found a great increase in the *Cxcr5* and *Il21* transcripts in the aged lymphoid organs (Fig. 4B). A similar pattern was observed for *Maf*, which activates the promoter and enhancer of *Il21* [56]. Interestingly, we also observed an increased expression of *Ikzf2* and *Prdm1* (encoding Helios and the B lymphocyte–induced maturation protein 1 (Blimp-1), respectively) in aged lymphoid organs. Although these genes participate in the differentiation of T_{fh} cells, they have a broader role in the regulation of function of effector T lymphocytes [57].

Taking into account the predominance of transcripts related to activation and effector memory among the $CD4^+$ non-Tregs in elderly mice, we then sorted out the genes related to Th1 and Th17 immune responses. Aged lymphoid organs were enriched in genes associated with highly differentiated Th1 cells (Fig. 4C), remarkably the upregulation of *Tbx21* and the downregulation of the second chain of the IFN-γ receptor (*Ifngr2*). Downregulation of the IFN-γ receptor is a hallmark of Th1 cells [58]. Some genes implicated in the development and maintenance of Th17 cells, such as *Rorc*, were also upregulated (Fig. 4C). *Card9*, an adaptor molecule that has shown to be required to mount adaptive Th1/Th17 responses, was greatly downregulated [59].

Then, we selected three DEGs (*Ccr5*, *Eomes*, and *Tbx21*) to validate our NanoString® results in lymphoid tissues and lacrimal glands with aging using flow cytometry. Cells expressing CCR5 are expanded in frail individuals [60]. Among other markers, high expression of *Eomes* and *Tbx21* is involved in $CD4^+$ T cell exhaustion [61]. Interestingly, opposite to the NanoString® results (Fig. 4D), flow cytometry analysis showed that CCR5 was not upregulated in the surface of conventional $CD4^+$ T cells in the aged spleen and it was significantly decreased in the aged CLN (Fig. 4E). We hypothesized that this discrepancy between the NanoString® and flow cytometry results is related to the shedding of the molecule in microvesicles as it has been previously demonstrated [62]. However, CCR5 was significantly increased in the aged compared to the young lacrimal glands (Fig. 4E). Intracellular expression of EOMES was highly increased in aged lymphoid organs and lacrimal glands while intracellular Tbet expression was increased in the aged lacrimal gland and spleen. We observed an increase in $EOMES^{dim}$ as well as $EOMES^{high}$ $CD4^+$ T cell subpopulations in the aged compared to the young lacrimal gland (Fig. 4F). High expression of EOMES is associated with exhaustion, mainly in $CD8^+$ T cells [61]. Although the frequency of $Tbet^+$ cells was higher in the aged lacrimal gland (Fig. 4E), we also observed a decrease in the Tbet MFI expression in $CD4^+$ T cells in the elderly lacrimal gland (Fig. 4G), a phenotype associated with poor proliferative capacity and preferential accumulation in the tissues [63]. Interestingly, we also observed increasing amounts of $CD4^+$IFN-γ^+Tbet^{neg} cells in the aged lacrimal gland (Fig. 4H), a phenotype related to immunopathology [64].

In conclusion, we found conventional T cells (non-Tregs) in aged lymphoid organs with an aberrant phenotype, characterized by activation, follicular helper markers, increased expression of inhibitory molecules, and transcription factors suggesting exhaustion and Th1-skewed effector memory cells. This

phenotype seems to be recapitulated in the aged lacrimal gland.

Naïve T cells accumulate in the aged lacrimal gland as compared to lymphoid organs

In elderly mice and also in humans, there is a shift in the T cells that populate the lymphoid organs compared to the young counterparts, from a predominant naïve to a more effector memory phenotype [2]. Our results in Fig. 4 demonstrated enrichment in DEGs related to an effector memory and highly differentiated phenotype in $CD4^+$ T conventional cells. We corroborated these findings by flow cytometry by staining $CD4^+$ T cells with CD62L and CD44 to identify naïve ($CD62L^+CD44^{neg}$), central memory (CM, $CD62L^+CD44^+$), effector memory (EM, $CD62L^{neg}CD44^+$), and effector-activated (EA, $CD62L^{neg}CD44^{neg}$) cells, analyzing lacrimal glands, CLN, and spleen separately (Fig. 5A, 5B). In aged spleen, we observed a shift in the distribution of the $CD4^+$ T cell subpopulations, from naïve towards effector memory T cell predominance. In this organ, central memory cell compartment also shrank in the aged group whereas effector-activated subpopulations appeared. The shift from naïve towards the effector memory phenotype was more pronounced in the CLN. Interestingly, we found a different $CD4^+$ T cell distribution in the lacrimal gland, with high proportions of effector memory cells in young and aged animals, but a remarkable increase in cells with the naïve phenotype.

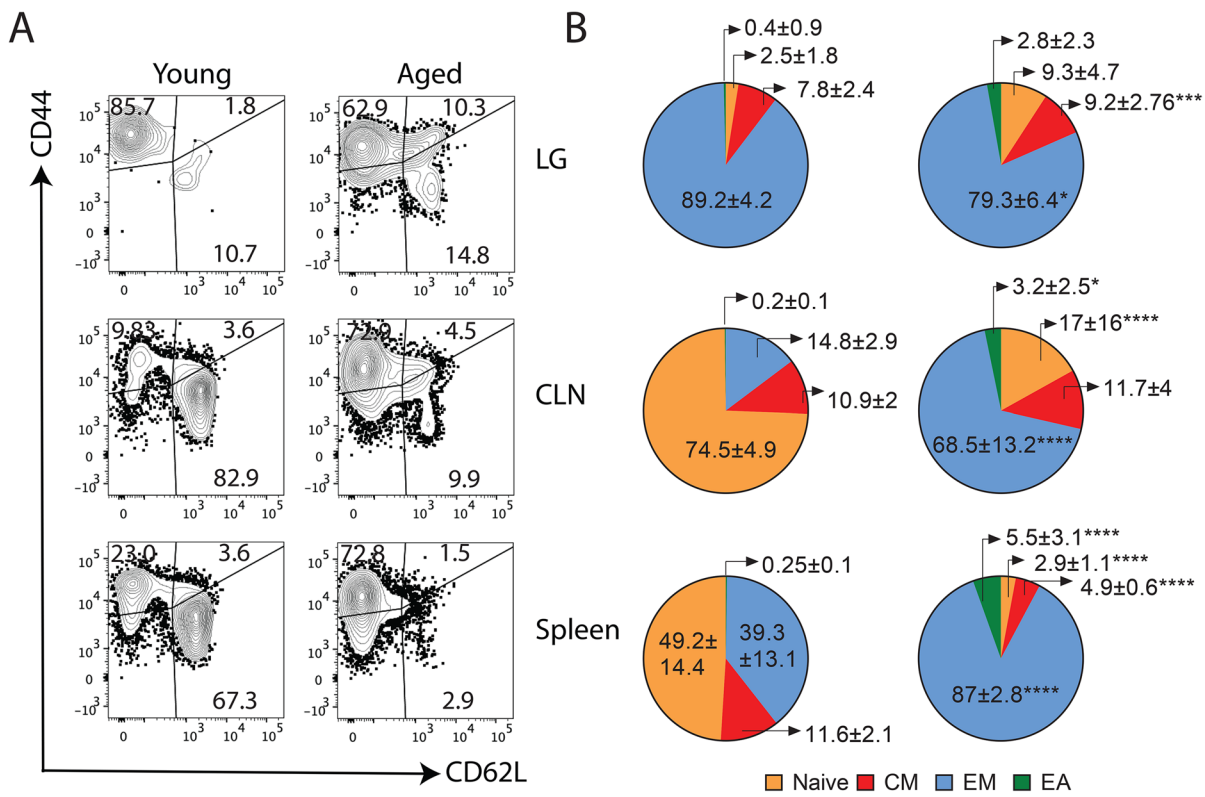

Fig. 5 Changes in the $CD4^+$ T cell signature in the lacrimal gland as compared to those from lymphoid tissues. **A** Representative contour plot from the different populations of $CD4^+$ T cells in the lacrimal gland (LG), draining cervical lymph nodes (CLNs) and spleen as measured by the expression of CD62 ligand (CD62L) and CD44. Numbers in the quadrants indicate the percentages of the different populations in alive $CD45^+CD3^+CD4^+$ cells in young and aged mice. **B** Pie charts depicting the average of the different $CD4^+$ T cell populations (naïve: $CD62L^+CD44^{neg}$, central memory (CM): $CD62L^+CD44^+$, effector memory (EM): $CD62L^{neg}CD44^+$, effector activated (EA): $CD62L^{neg}CD44^{low}$) from the different tissues ($n=5$ animals/group) in young and aged mice. Numbers indicate the means ± standard deviation of the different populations. $^*p<0.05$, $^{**}p<0.01$, $^{***}p<0.001$; $^{****}p<0.0001$. Values expressed as mean ± standard deviation. Statistical significance based on the Mann–Whitney *U* test

These findings demonstrate differential distribution of the CD4$^+$ T cells in the aged lacrimal gland as compared with that in the aged lymphoid tissues.

A highly activated and effector memory Treg phenotype in aged lymphoid organs may not be sufficient to control the highly experienced and exhausted CD4$^+$ T conventional cells

The effect of aging on the ability of Tregs to suppress or not suppress has been investigated previously, although no final consensus exists. Harpaz et al. [65] have shown that Tregs isolated from spleen, either from young and aged mice, are able to suppress T effector cells from young mice but they fail to do so when they are confronted to aged T effector cells, likely due to an intrinsically dysregulated expression of genes related to T cell activation and regulation in the later cells. Our results demonstrated that Tregs from aged lymphoid organs are highly activated effector memory Tregs that express IFN-γ and IL-17A, a phenotype that affect their suppressive function against effector cells [42]. Likewise, our NanoString® and flow cytometry analysis suggested that conventional (non-Tregs) cells are highly exhausted and possess a phenotype related to immunopathology. In order to characterize the functional potential of Tregs in relation to those non-Tregs in aged lymphoid organs, we calculated the ratio of DEGs in aged Tregs versus aged non-Tregs and then compared this list with the one when we confronted in silico aged Tregs versus young non-Tregs (Supplementary Table 3).

Approximately 23% (22/96 genes) of the DEGs from the aged Tregs versus aged non-Tregs were exclusively expressed in this pair as compared with aged Tregs versus young non-Tregs (Fig. 6A). From them, only three genes were upregulated in aged Tregs and among them was *Itga5*, encoding the integrin alpha 5. Interestingly, loss of integrin activation in Tregs leads to systemic autoimmunity [66]. The remaining 20/23 genes were downregulated in aged

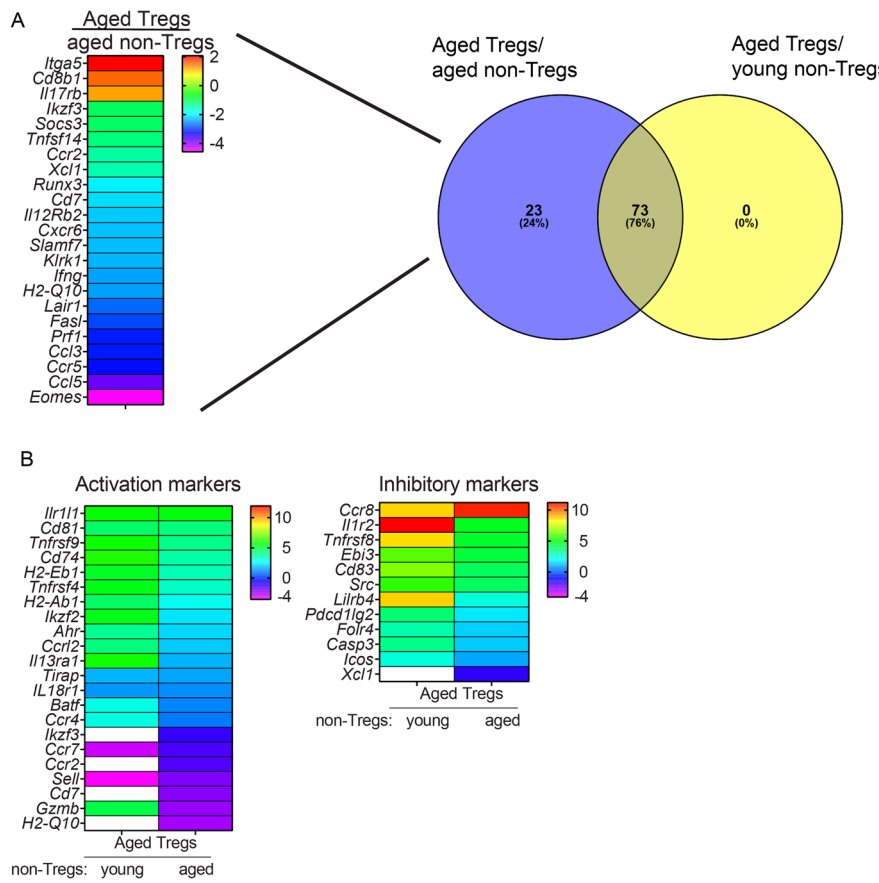

Fig. 6 Comparative multiplex analysis of the mRNA for immune-related genes in Tregs versus non-Tregs with aging. RNA was isolated from sorted Tregs and non-Tregs from a mixture of draining cervical lymph nodes (CLNs) and spleen of young and aged mice ($n = 5$–7 biological replicates/group) and subjected to NanoString® analysis using the immunology panel v2. **A** The number of differentially expressed genes (DEGs) in aged Tregs versus aged non-Tregs as compared to aged Tregs versus young non-Tregs is shown in a Venn diagram, depicting in the heatmap those that were only present in the aged pair. **B** DEGs either related to activation or inhibitory function are shown in the left and right heatmaps, respectively. White boxes indicate no statistical significance in that pair

Tregs as compared to aged non-Tregs, and among them were several associated with cytotoxic T cell responses (*Xcl1*, *Slamf7*, *Ccl3*) [49, 67, 68].

Among the shared DEGs between aged Tregs and aged non-Tregs as compared with aged Tregs versus young non-Tregs, many were activation markers. Interestingly, most of those activation markers (except for *Il1rl1*, *Tirap*, and *Il18r1*) exhibited greater fold expression in aged Tregs versus young non-Tregs (Fig. 6B). The same pattern was observed for several inhibitory markers but *Ccr8* that was similarly expressed in both pairs (Fig. 6B).

These observations suggest that aged Tregs from lymphoid organs are licensed to exert their suppressive function, but they might be insufficient to control the activation and exhaustion phenotype of aged non-Tregs with increased expression of inhibitory transcripts. Whether this is recapitulated in the lacrimal gland is not clear yet.

Aged Tregs are less responsive while aged Tresponders are overly active

After identifying such profound changes in the transcriptome of aged Tregs and non-Tregs as compared with their young counterparts, we performed two different functional assays to investigate their function in lymphoid organs. In the first, we performed a Treg suppression assay in which either young or aged non-Tregs (Tresponders) were stimulated to proliferate in vitro in the presence of either young or aged Tregs. For this assay, we isolated Tresponders ($CD4^+CD25^-$ cells) and Tregs ($CD4^+CD25^+$ cells) from lymphoid organs using magnetic beads and co-cultured them for 72 h in anti-CD3-coated plates. Proliferation as measured by WST assay demonstrated that young and aged Tresponders had similar proliferative capacity, while aged Tregs proliferated more than young Tregs (Fig. 7A). As expected, young Tregs decreased young Tresponder proliferation, but this effect was considerably weaker on aged Tresponders. Crossover studies showed that while aged Tregs could partially suppress the proliferation of young Tresponders, this effect was lost on aged Tresponders.

We also measured the production of IFN-γ and IL-17 in the supernatants of the same cultures using the immunobead assay. Aged Tresponders produced greater amounts of IFN-γ and IL-17 than young Tresponders, in agreement with our NanoString® results and the findings by Harpaz et al. [65]. Also, in agreement with our NanoString® and flow cytometry results, a significant increase in IFN-γ levels in the culture supernatants was also observed in aged Tregs, albeit in a lesser extent than the amount produced by Tresponders (Fig. 7B). Young Tregs could suppress IFN-γ production by Tresponders, while aged Tregs failed to do so, irrespective of the responder cell age (Fig. 7B). Interestingly, there was an additive effect on IL-17 production when aged Tresponders were co-cultured with aged Tregs that reached statistical significance (Fig. 7A).

Activated conventional T cells might also transiently upregulate CD25. This might represent a confusing factor for the Treg suppression assay, when trying to isolate Tregs based only on the expression of this marker (Fig. 7A) [69]. Therefore, we evaluated the capacity of young and aged Tregs to suppress $CD4^+$ T cell proliferation, isolating Tregs based on the expression of CD25 and GITR as shown in Supplemental Fig. 1. To this purpose, Tregs ($CD4^+CD25^+GITR^+$) and non-Tregs ($CD4^+CD25^{neg}GITR^{neg}$) were first sorted from lymphoid organs of young and aged mice and then mixed at different ratios with CellTrace™ Violet–labeled $CD4^+$ T splenocytes isolated from young mice (Tresponders). Tresponders were cultured in CD3 antibody–coated plates for 3 days to induce T cell activation, and then, their proliferation was evaluated using dye dilution by flow cytometry. As depicted in Fig. 7C, the addition of increasing numbers of young Tregs led to reduced proliferation of the Tresponders in the presence of a strong activation stimulus, whereas the addition of the same numbers of aged Tregs did not have such effect.

Overall, these results demonstrate that aged Tregs from lymphoid organs have markedly impaired suppressive capacity, whereas aged Tresponders have dysregulated proliferative and cytokine-producing properties. Experiments are ongoing in our laboratory to evaluate the functionality of $CD4^+$ T cells from the mouse aged lacrimal gland.

Aged human lacrimal glands are infiltrated with $CD3^+$, $CD20^+$, and $CD4^+Foxp3^+$ cells

Animal models are very helpful to characterize the different players of the immune system in the process of immunosenescence. However, a plethora of factors, either genetic, environmental, or infectious,

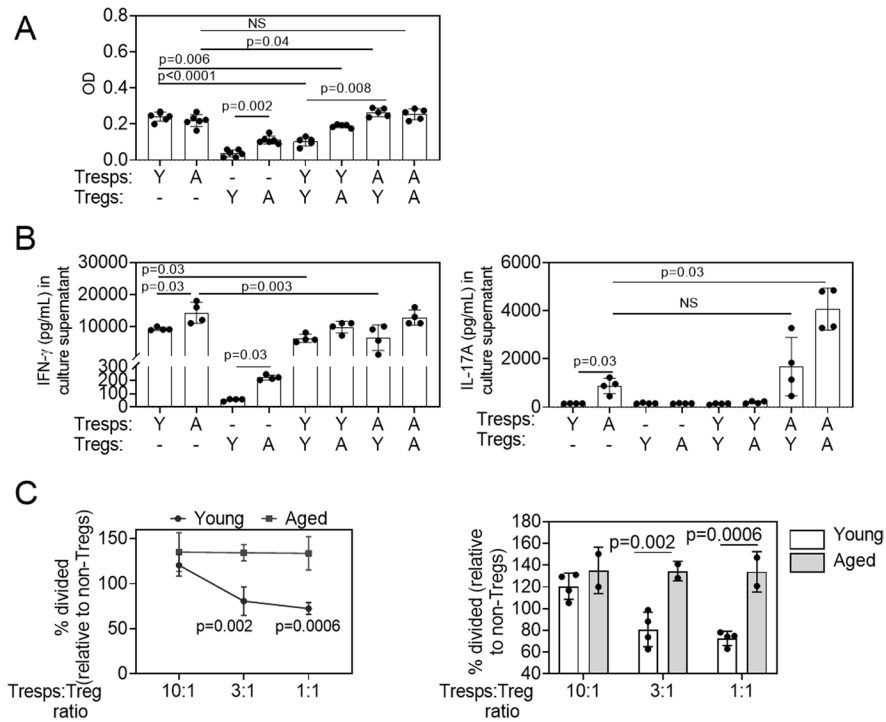

Fig. 7 Aged regulatory T cells do not suppress well in vitro, and aged T responders are overly active. **A** Cell proliferation was measured for young and aged $CD4^+CD25^{neg}$ Responders (Tresps) and young and aged $CD4^+CD25^+$ Tregs using the colorimetric WST-1 Cell Proliferation Reagent. Tregs and Tresps were cultured at a 1:1 ratio for 72 h in a plate previously coated with CD3/CD28 as described in the "Methods." Bar graphs show means ± SD of data combined from two independent experiments (four to five mice were pooled/age/experiment). One-way ANOVA followed by Dunnett's multiple comparison test. **B** The production of IFN-γ and IL-17A was determined in culture supernatants by the Luminex assay. Co-culture supernatants were collected in triplicate from two independent experiments. Bar graphs show means ± SD of data combined from two independent experiments (four to five mice were pooled/age/experiment). The Mann–Whitney *U* test was used to compare specific pairs. NS = non-significant. **C** Cell proliferation was measured for $CD4^+$ Responders in the presence of young and aged $CD4^+CD25^+GITR^+$ Tregs or $CD4^+CD25^{neg}GITR^{neg}$ non-Tregs using Violet Tracer staining followed by flow cytometry. Tregs/non-Tregs and Responders were cultured at different ratios for 72 h in a plate previously coated with anti-CD3 antibody as described in the "Methods." The percentage of cell division was calculated based on the Responder proliferation. Data are shown both as suppression curves and bar graphs. Two-way ANOVA followed by Sidak's multiple comparison test

influence human aging, particularly in the ocular surface, that might be very different to mice. To address this gap in knowledge, we examine human lacrimal glands that were obtained from cadavers. In aged human lacrimal glands, several authors have demonstrated lymphocytic infiltration that correlates with gland pathology and acinar atrophy together with differential expression of mucins [70–73] but it remains unclear if $CD4^+Foxp3^+$ cells are also present. In this study, human lacrimal glands from five cadavers (age range 55–81 years, 3 females, 2 males) were examined by hematoxylin and eosin staining to verify their normal structure. Unlike the murine lacrimal gland, the acini were loosely arranged and surrounded by loose connective tissue (not shown). To characterize the B and T lymphocytes, immunohistochemical antibody reactions were performed using anti-CD20 and anti-CD3 antibodies. B cells were detected in the lacrimal gland as single cells and as cell clusters, mostly compactly arranged (Fig. 8A). The number and size of the B cell clusters differed between the lacrimal glands examined, but they were associated with a T cell zone in all cases (Fig. 8B, C). In some cases, the structure of a follicle with a typical B cell and T cell zone could be seen; however, such accumulations were rarely arranged in a typical

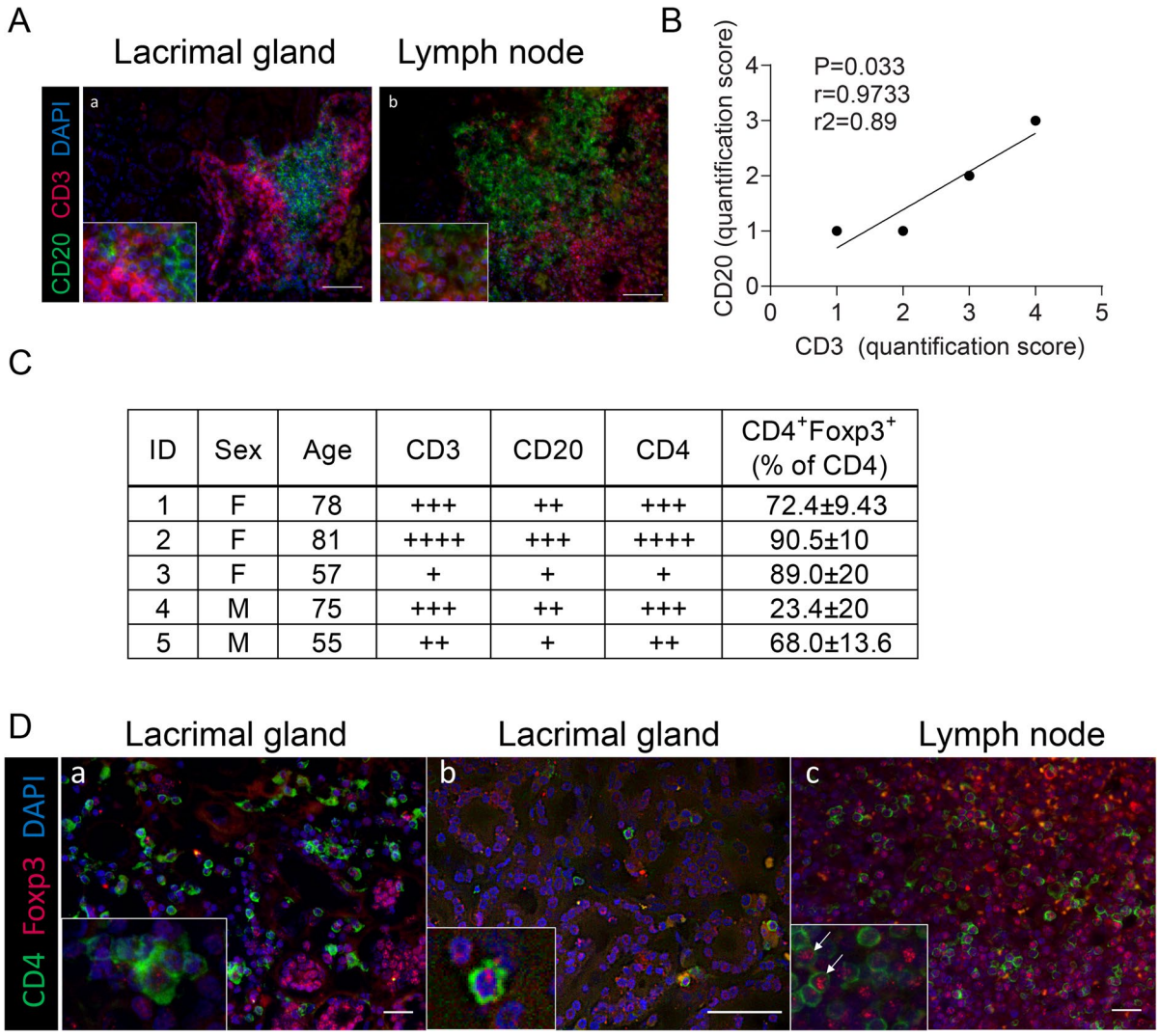

C

ID	Sex	Age	CD3	CD20	CD4	$CD4^+Foxp3^+$ (% of CD4)
1	F	78	+++	++	+++	72.4±9.43
2	F	81	++++	+++	++++	90.5±10
3	F	57	+	+	+	89.0±20
4	M	75	+++	++	+++	23.4±20
5	M	55	++	+	++	68.0±13.6

Fig. 8 Aged human lacrimal glands have infiltration with $CD3^+$, $CD20^+$, and $CD4^+Foxp3^+$ cells. **A** Representative merged image of human lacrimal gland (a) and lymph node (b) immunostained with anti-CD3 (T cells, red) and anti-CD20 (B cells, green) antibodies with DAPI nuclear counterstaining (blue). **B** Spearman's correlation of T and B cell infiltration scores. *r* coefficient of correlation, r^2 coefficient of determination. **C** Demographics of lacrimal glands used and the corresponding infiltration scores, as described in the "Methods." **D** Representative merged images of human lacrimal gland (a, b) and lymph node (c) immunostained with anti-CD4 (green) and Foxp3 (red) antibodies with DAPI nuclear counterstaining (blue). Magnification 400-fold and in the small squares, magnification 600-fold; scale bar = 50 μm

manner nor could we detect high endothelial venules. $CD3^+$ T cell groups gave a more scattered impression. There were also T cell assemblies that were not associated with B cells. In addition to clusters, T and B lymphocytes were also detectable as single cells in between acini, as described in previous studies [74–77]. Overall, there were more T cells than B cells. A significant positive Spearman's correlation between the proportion of T cells and B cells was also observed (Fig. 8B).

Next, we further characterize the $CD3^+$ T cells by performing double immunofluorescence using anti-CD4 and anti-Foxp3 antibodies in these aged lacrimal glands. Lymph nodes were used as positive controls (Fig. 8C, D). As observed for $CD3^+$ T cells, $CD4^+$ T cells were detected as single cells between acini and

as cell clusters (Fig. 8D). The quantification of $CD4^+$ T cells revealed a similar portion as for $CD3^+$ T cells, suggesting that mainly $CD4^+$ T cells were infiltrating the aged human lacrimal glands (Fig. 8C). Furthermore, our analysis showed that many of the $CD4^+$ T cells located as single cells between the acini were also Foxp3 positive. In contrast, few $CD4^+$ T cells located in a cell cluster were $Foxp3^+$.

Our results agree with the literature about the presence of CD3 and B cells in aged human lacrimal glands. However, for the first time, the presence of $CD4^+Foxp3^+$ cells was also observed.

Methods

Animals

The Institutional Animal Care and Use Committees at Baylor College of Medicine and the Jackson Laboratory approved all animal experiments (approval number AN-7342). All studies adhered to the Association for Research in Vision and Ophthalmology for the Use of Animals in Ophthalmic and Vision Research and to the National Institutes of Health Guide for the Care and Use of Laboratory Animals (NIH Publications No. 8023, revised 1978). The experiments were performed at the Ocular Surface Center, Department of Ophthalmology, Baylor College of Medicine (Houston, TX, USA), and at the Jackson Laboratory (Bar Harbor, ME, USA).

Breeder pairs of 6–8-week-old C57BL/6J mice were purchased from the Jackson Laboratory (Bar Harbor, ME, USA) for establishing breeder colonies. Naturally, aged female C57BL/6J mice were maintained in specific pathogen-free vivarium and were used at 22–26 months ($n=43$). Young mice ($n=46$) and middle-aged mice ($n=5$) were used at 2–3 months and 12–13 months, respectively. Because dry eye disease is more frequent in women [6] and aged male mice do not develop corneal barrier disruption (a hallmark of dry eye disease) [78], only female mice were used in our experiments.

Mice were housed in specific pathogen-free facilities of Baylor College of Medicine and Jackson Laboratory and were kept on diurnal cycles of 12-h light and 12-h dark with ad libitum access to food and water and environmental enrichment. No intervention was made to the mice, and therefore, our experiments did not induce pain, suffering, or distress to the animals. Criteria for early euthanasia included loss of 20% or more of body weight, extensive ulcerative dermatitis, or corneal opacification. Mice subjected to early euthanasia were not included in the study.

Flow cytometry analysis

Extraorbital lacrimal glands were excised and processed into single cell suspension as previously described [20]. Single cell suspensions from eye-and-lacrimal gland draining CLN and spleens from the different groups of mice were prepared by teasing the tissues previously resuspended in complete RPMI (RPMI [Thermo Fisher Scientific, Waltham, MA] + 10% fetal bovine serum [HyClone, Logan UT] + 1% penicillin/streptomycin [HyClone]) through a nylon mesh (Tisch Scientific, North Bend, OH, USA) in petri dishes and discarding the cell debris. Red blood cells were lysed by using the ammonium chloride Tris buffer, and leukocytes were counted using a hemocytometer under a dissection microscope and resuspended at 1×10^7 cells/mL. For intracellular cytokine staining, 1×10^6 cells/well was incubated in round-bottom 96-well plates with PMA (100 ng/mL, Sigma, Saint Louis, MO, USA) and ionomycin (1 µg/mL, Sigma) in 100 µL complete RPMI 1640 for 6 h at 37 °C, with 5% CO_2. In the last 2 h of incubation, 1 µL GolgiStop™ (BD Biosciences, Franklin Lakes, NJ, USA) in 50 µL complete RPMI was added to the wells. Fc receptors were then blocked with the anti-mouse CD16/32 antibody (BioLegend, San Diego, CA, USA) followed by surface staining with the antibodies anti-CD45_Bv510 (Clone 30-F11, BioLegend), anti-CD3ε_BB700 (Clone 145-2C11, BD), anti-CD4_FITC (Clone RM4-5, Thermo Fisher), anti-CD25_PE (Clone HT-2, BD), anti-CD121b_BV421 (Clone 4E2, BD), anti-CD81_BV421 (Clone Eαt2, BD), anti-CD44_APC (Clone IM7, BioLegend), anti-CCR5_BV421 or anti-CCR5_PE (Clone C34-3448, BD), and anti-CD62L_BV421 (Clone MEL-14, BioLegend) for 20 min. Afterwards, cells were incubated with an infrared fluorescent reactive dye diluted 1:32 (Thermo Fisher) for 10 min, washed, and resuspended in the fixation/permeabilization buffer from the Transcription Factor Buffer Set (BD) for 18 h. Cells were then washed with 1× of the perm/wash buffer from the same set and stained with anti-Foxp3_PE-Cy7 (Clone FJK-16 s, Thermo Fisher), anti-Tbet_PE-Cy7

or anti-Tbet_APC (Clone 4B10, BioLegend), anti-EOMES_PE (Clone X4-83, BD), anti-IL-17_PE (Clone eBio17B7, eBioscience), and anti-IFN-γ_ Pacific Blue (Clone XMG1.2, BioLegend), according to the panel design. The following gating strategy was used in this study: cells were identified by forward scatter area versus side scatter area; doublets were discriminated by forward scatter height versus forward scatter area (singlet 1) followed by side scatter height versus side scatter area (singlet 2); thereafter, dead cells were excluded by gating live fixable infrared dye versus side scatter; subsequently, $CD45^+$ cells were gated and then either $CD3^+CD4^+$ or $CD4^+$ cells were selected to calculate the frequency of the extracellular or intracellular markers in the different combinations. Frequency of cells is shown as a percentage of $CD45^+$ cells.

Negative controls consisted of fluorescence minus one (FMO) splenocytes. Cells were acquired with the BD Canto II Benchtop cytometer with BD Diva software version 6.7 (BD Biosciences). Final data were analyzed using FlowJo software version 10 (Tree Star, Inc., Ashland, OR, USA).

Flow cytometry sorting and NanoString® analysis

$CD4^+$ T cells were enriched from CLN and spleen suspensions by using the $CD4^+$ T cell isolation kit (Miltenyi Biotec, Auburn, CA, USA) following the manufacturer's instructions. Either young or aged lymphoid tissues from three mice per age were pooled as one sample. After blocking Fc receptors (BioLegend), enriched cells were stained with the antibodies anti-CD4_FITC (Clone RM4-5, Thermo Fisher), anti-CD25_PE (Clone HT-2, BD), and anti-GITR_APC (Clone DTA-1, BioLegend). Dead cells were stained prior to cell sorting by using fixed cell ready DAPI (Thermo Fisher) following the manufacturer's instructions. $CD4^+CD25^+GITR^+$ (Tregs) and $CD4^+CD25^{neg}GITR^{neg}$ (non-Tregs) cells were sorted on a FACSAria II cytometer (BD), and then, pellet was obtained to resuspend it in the Buffer RLT Plus (Qiagen, Hilden, Germany) + β-mercaptoethanol 1:100 (Bio-Rad, Hercules, CA, USA) and frozen immediately at − 80 °C. Post-sorting analysis indicated between 85 and 99% purity (Supplemental Fig. 1). These experiments were performed either at Baylor College of Medicine (3 young and 3 aged samples) or Jackson Laboratory (4 young and 3 aged samples), yielding a sample size of 7 young and 6 aged independent samples from Treg and non-Treg populations, respectively. Total RNA was isolated using a RNeasy Mini Kit (Qiagen) following the manufacturer's protocol. The RNA concentration was measured by its absorption at 260 nm using a spectrophotometer (NanoDrop 2000, Thermo Fisher Scientific) and Agilent Bioanalyzer. Biological replicates containing at least 70 ng RNA were used to run NanoString® at the Genomic and RNA Profiling Core from Baylor College of Medicine. Data was then analyzed using nSolver® (version 4.0) and ROSALIND® software.

NanoString® data analysis using ROSALIND®

Five hundred forty-three transcripts were quantified with the NanoString® nCounter multiplexed target platform using the Mouse Immunology V2 panel (www.nanostring.com). nCounts of mRNA transcripts were normalized using the geometric means of 14 housekeeping genes (*Gapdh*, *Gusb*, *Ppia*, *Hprt*, *Tbp*, *Tubb5*, *G6pdx*, *Alas1*, *Sdha*, *Oaz1*, *Polr1b*, *Polr2a*, *Rpl19*, *Eef1g*). Data was analyzed with a HyperScale architecture developed by ROSALIND®, Inc. (https://rosalind.onramp.bio/) (San Diego, CA, USA). Read distribution percentages, violin plots, identity heatmaps, and sample MDS plots were generated as part of the QC step. Normalization, fold changes, and *p* values were calculated using criteria provided by NanoString®. ROSALIND® follows the nCounter Advanced Analysis protocol of dividing counts within a lane using the same lane's geometric mean of the normalizer probes. Housekeeping probes to be used for normalization are selected based on the geNorm algorithm as implemented in the NormqPCR R library [79]. The abundance of various cell populations is calculated on ROSALIND® using the NanoString® Cell Type Profiling Module. ROSALIND® performs filtering of cell type profiling results to include results that have scores with a *p* value smaller than or equal to 0.05. Fold changes and *p* values are calculated using the fast method described in the nSolver® Advanced Analysis 2.0 User Manual. *p* value adjustment is performed using the Benjamini–Hochberg method of estimating false discovery rates (FDRs). Clustering of genes for the final heatmap of differentially expressed genes was done using the partitioning around medoids (PAM)

method using the FPC R library [80] that considers the direction and type of all signals on a pathway, the position, role, and type of every gene. Hypergeometric distribution was used to analyze the enrichment of pathways, gene ontology, domain structure, and other ontologies. The topGO R library [81] was used to determine local similarities and dependencies between GO terms to perform Elim pruning correction. Several database sources were referenced for enrichment analysis, including Interpro [82], NCBI5 [83], MSigDB [84, 85], REACTOME [86], and WikiPathways [87]. Enrichment was calculated relative to a set of background genes relevant for the experiment. Data analyzed in ROSALIND® was downloaded, and volcano plots of differential expression data were plotted using the $-\log^{10}$ (p value) and $\log^2$ fold change using GraphPad Prism. Heatmaps were also constructed using GraphPad Prism. Venn diagrams were made using Venny 2.1 [88].

Imaging cytometry

Imaging cytometry was completed using an ASSIST-calibrated ImageStreamX Mark II (EMD Millipore-Amnis Corp., Seattle, WA, USA) equipped with blue (200 mW, 488 nm), yellow–green (200 mW, 561 nm), red (150 mW, 642 nm), and violet (120 mW, 405 nm) lasers and a side scatter far red (70 mW, 785 nm). The same antibodies described above were used. Images were acquired using the Inspire acquisition software (Ver. 200.1.388.0) and utilizing the 40×objective (Multimag option, 60×, 40×, and 20×objectives). Raw image files (.rif) were acquired and adjusted for spectral overlap post-acquisition using the IDEAS analysis software (Ver. 6.2.64.0). Prior to the assay, single-color control tubes were collected with no bright-field illumination and no SSC laser and were used to create a compensation matrix in IDEAS. The matrix was applied to.rif files to generate a compensated image file (.cif) for each sample. Single cells were selected using the shape change wizard–guided analysis tool creating a focus (Gradient RMS of the Bright field), cells (Aspect Ratio_M01 versus Area_M01), live (Intensity_Ch12), and single circular (Circularity_Object [M01,1-BF.Tight]). Cellular populations of interest were then selected through gating $CD45^+$, $CD4^+$, $Foxp3^+$, $IL17^+$, and IFN-γ^+ cells, followed by visual inspection of the images to further refine gates.

Treg suppression assay using isolation based on CD4 and CD25 expression

$CD4^+CD25^{neg}$ cells ("Tresponders") and $CD4^+CD25^+$ cells ("Regulatory T cells," Tregs) were isolated from pooled CLN and spleens from young or aged mice using a T regulatory isolation Kit (Miltenyi), according to the manufacturer's instructions. Cells were co-cultured at Tresponders:Tregs 1:1 ratio (1×10^5:1×10^5 cells) or alone in an anti-CD3 antibody-coated 96-well plate for 72 h. The assay was set up with four wells per experimental group. A colorimetric WST-1-based (Abcam) proliferation assay was performed by adding 10 µL of this reagent per 100 µL of culture media and incubated for at least 8 h of the co-culture period, as previously reported. Supernatants were collected and stored at − 80 °C until ready to use. Results presented are the combined results of two independent experiments.

Multiplex cytokine immunobead assay (Luminex)

Culture supernatants were collected from the WST-1-based assay, and cytokine production was determined by Luminex assay. Samples were added to wells containing the appropriate cytokine bead mixture that included mouse monoclonal antibodies specific for IFN-γ or IL-17A (Upstate-Millipore, Billerica, MA, USA) as previously reported. The reactions were detected with streptavidin–phycoerythrin using a Luminex 100 IS 2.3 system (Austin, TX, USA). Results presented are the combined results of two independent experiments.

In vitro Treg suppression assay using isolation based on CD4, CD25, and GITR

$CD4^+$ T cells were isolated from murine splenocytes with $CD4^+$ T Cell Isolation Kit (Miltenyi), then labeled with CellTrace Violet Cell Proliferation Kit following the manufacturer's instructions and finally used as responder T cells. Consecutively, splenocyte-depleted cell suspensions were prepared with the aid of a CD3 depletion kit (Miltenyi) following the manufacturer's instructions and used as antigen-presenting cells. In parallel, $CD4^+$ T cells were isolated from pooled splenocytes and cervical lymph node cells and then labeled with anti-CD25 and anti-GITR as described above and sorted into

two fractions: Tregs ($CD4^+CD25^+GITR^+$) and non-Tregs ($CD4^+CD25^{neg}GITR^{neg}$). At least 2×10^6 cells were sorted for each experiment from 5 young mice per group and 2–3 aged mice per group. Finally, Tresponder cells and either sorted non-Tregs or Tregs were co-cultured at a final concentration of up to 1×10^6 cells/mL in the presence of previously CD3 plate–bound (1 µg/mL). After 72 h in culture, cells were labeled with anti-CD4 and viability dye and analyzed by flow cytometry. The percentage of cell division was calculated in relation to non-Tregs of the same age.

Human samples and immunohistochemistry

Human lacrimal glands were obtained from 5 cadavers (aged 65–89 years, 3 females, 2 males) donated to the Institute of Anatomy, FAU Erlangen Nürnberg, Germany, by will and free of recent trauma, ocular or nasal infections, or diseases affecting or interfering with lacrimal gland function and were used in accordance with the Declaration of Helsinki. A history of dry eye disease cannot be excluded in these cases. Lacrimal glands were carefully dissected to clearly exclude contamination with conjunctival tissue. Hematoxylin and eosin staining was used to verify structure, and immunofluorescence staining was used to characterize lymphocyte populations in aged human lacrimal gland in paraffin-embedded sections. (5 µm). Briefly, deparaffinized and rehydrated sections were subjected to antigen retrieval in 1 mM ethylenediaminetetraacetic acid (EDTA) buffer (pH 9.0) for 10 min at 80 °C and then treated with trypsin (1 mg/mL; Sigma-Aldrich, Germany) for 10 min at 37 °C in a humidity chamber. Non-specific binding was blocked with Blotto (10 mg/mL skimmed milk powder in PBS-T). According to the staining panel, the following primary antibodies were applied overnight at 4 °C: rabbit polyclonal anti-CD3 (1:50; Dako, Santa Clara, CA, USA), mouse anti-CD20 (undiluted, clone L26, Dako), rabbit monoclonal anti-CD4 (1:100, Abcam, Cambridge, UK), and mouse anti-Foxp3 (1:50, clone 2A11G9; Santa Cruz, Dallas, TX, USA). Sections were then incubated with the Alexa Fluor 555 or Alexa Fluor 488–conjugated secondary antibodies at a 1:500 dilution (Thermo Fisher), followed by counterstaining with DAPI for 3 min. To verify the staining procedure, human lymph nodes were used as positive controls. Positively stained cells were detected at 400-fold magnification with a microscope (DM4000 B; Leica, Germany) and quantified as follows: +, few individual cells; ++, few individual cells and additional one/few cell clusters; +++, few individual cells and several cell clusters; and ++++, few individual cells and many cell clusters. Within the subset of $CD4^+$ T cells, the amount of $Foxp3^+$ T cells was analyzed in seven randomly selected field-of-views (242.73×182.05 µm) in 600-fold magnification using a Keyence BZX800E microscope (Osaka, Japan).

Statistics

Statistical analyses were performed with GraphPad Prism (GraphPad, Inc., version 9). Non-parametric Mann–Whitney *U* tests were used to make comparisons between two age groups. All experiments were repeated at least once, and representative experiments are shown. Spearman's non-parametric correlation was used to evaluate the correlation between CD3 and CD20 quantification scores. No experimental units were excluded during the analysis. Since this was an exploratory study, no sample size calculation was performed. No randomization or blinding was used to allocate experimental units. Co-founders were not controlled in these experiments.

Discussion

Immunosenescence in the different tissues of the body is a very intricate process, involving several branches of the immune and inflammatory responses, at the molecular and cellular levels [3]. Aged $CD4^+$ T cells as helper mediators of immunity are at the epicenter of this process, responsible for perpetuating damage and organ dysfunction [89]. This landscape is particularly important for the lacrimal gland, on which age-related dysfunction alters the lacrimal functional unit, adding complexity to conditions such as KCS and SS [6]. In the present study, we aimed to characterize the immune phenotype of aged $CD4^+$ T cells, with a special focus on the lacrimal gland as compared to the lymphoid organs. We confirmed that percentages of Tregs increased with aging not only in CLN and spleen but also in the lacrimal gland of C57BL/6J mice. In humans, we observed the formation of lymphocyte clusters resembling TLT structures in the

lacrimal gland of adults and we detected the presence of $CD4^+Foxp3^+$ cells in this tissue. Intriguing puzzles remain to be the mechanisms that induce the augmented percentages of Tregs and other lymphocytes to the glands and the formation of these TLT-like structures. Persistent oxidative stress and compromised autophagy may contribute to the induction of inflammation and immune cell activation with aging [3]. Our work has shown that dietary modulation of the antioxidant machinery in aged mice decreases inflammatory transcripts and levels of $CD45^+CD4^+$ cells in the lacrimal gland [9]. Once T cells have been recruited to the lacrimal gland, homeostatic proliferation might contribute to the invasion process [11]. In elderly individuals, thymic involution with the consequent loss of thymic-derived naïve T cells is partially compensated by homeostatic proliferation of naïve T cells generated in the periphery [90]. In agreement with this evidence, we found increased percentages of naïve $CD4^+$ T cells in the lacrimal gland of aged mice, as opposed to the lymphoid organs. At a slow rate, this process might occur in the absence of exogenous antigen and, instead, might be induced by self-antigen:MHC complexes on antigen-presenting cells [91]. However, exogenous antigens from pathogens such as cytomegalovirus have been shown to enhance the development of immunosenescence in humans [92], and increased Epstein–Barr virus infection is observed in patients with KCS [93].

According to our transcriptome analysis in lymphoid organs and the flow cytometry and live imaging in the lacrimal glands, several types of $CD4^+$ T cells might co-exist and expand in these tissues and the highly differentiated Tregs co-opt for the expression of the cytokines from the corresponding effector T cells that they target for suppression. Interestingly, Th1-like Tregs have also been observed in autoimmune-mediated pathologies such as multiple sclerosis and type 1 diabetes [42]. This also agrees with the results from Elyahu et al. [89] that used single-cell transcriptomic and flow cytometry investigation of aged splenocytes. They described a heterogeneous landscape in the T conventional and Treg pool in mouse spleen where cytotoxic, exhausted, and highly activated cells prevailed with aging [89]. However, It would be important to consider here that, as opposed to activated and effector T cells, naïve T cells are transcriptionally quiescent cells, so other methods beyond the measurement of the cell transcripts need to be employed in order to have a better picture of the immune populations that prevail with aging [94].

Our evidence suggested that non-Tregs also showed signs of immunopathology in the lacrimal gland; for example, we also observed increasing amounts of $CD4^+IFN\text{-}\gamma^+Tbet^{neg}$ cells. In the model of the *Toxoplasma gondii* infection, López-Yglesias et al. [64] showed T-bet-deficient Th1 cells mediate $IFN\text{-}\gamma^+$-dependent intestinal inflammation and parasite-driven loss of paneth cells. It would be interesting to ascertain if Tbet is dispensable for the development of T cell infiltration and dysfunction in the lacrimal gland with aging. The information of this analysis might shed light into the potential molecular targets to manipulate aged $CD4^+$ T cells. Some advances have been made in this regard. For example, pharmacological inhibition of *Entpd1*, encoding CD39, one of the DEGs in aged $CD4^+$ non-Tregs in our analyses, induced better responses to vaccination in the elderly [95]. Also, inhibition of RANKL prevents autoimmune inflammation in the central nervous system [96].

Another puzzling question in the process of lymphocyte invasion of the lacrimal gland is the functionality of highly mature aged $CD4^+$ T cells and their role in the modulation of inflammation in this organ. With regard to tissue Tregs, their presence in several tissues has been proven beneficial for the modulation of inflammation, although these studies did not focus on aged cells [34]. Of note, several studies have tried to evaluate the suppressive function of splenic Tregs confronted to conventional T cells from elderly mice by using the ex vivo Treg suppression assay; however, this method has technical caveats [97]. Moreover, we and other authors have used $CD4^+CD25^{high}$ cells to evaluate Treg function. However, mouse aged Tregs are heterogeneous in the expression of CD25 and, therefore, the results are still not conclusive, with some studies showing a decrease while others report an increase in suppressive capacity or no change [12, 14, 20, 98]. In the present study, we evaluated the suppressive capacity of $CD4^+CD25^+$ Tregs from aged lymphoid organs with a colorimetric assay and observed less ability to suppress proliferation and IFN-γ secretion of $CD4^+CD25^{neg}$ Tresponders as compared to their young counterparts. These results were confirmed by a flow cytometry–based Treg suppression assay using $CD4^+CD25^+GITR^+$ Tregs and $CD4^+CD25^{neg}GITR^{neg}$ T responders.

Interestingly, aged Treg function seems insufficient to suppress the effects of highly activated effector $CD4^+$ T cells and preferentially suppress IFN-γ compared to IL-17-producing T cells [65, 98]. As we compare the magnitude of the DEGs of aged Tregs versus aged non-Tregs and aged Tregs versus young non-Tregs, greater differences were observed in the fold increase of cytotoxic, activated, and inhibitory DEGs in the first pair. In this study, we also showed that aged T responders escape suppression from young Tregs, suggesting that an accumulation of responder cells with aging may lead to greater pathogenicity on a per cell basis, in agreement with the study by Harpaz et al. [65]. These results also support the inability of Tregs to control the function of non-Tregs with aging. However, aged Tregs might also possess some degree of defective function, as demonstrated by Morales-Nebreda et al. [99] in the mouse model of influenza. They observed that adoptive transfer of young Tregs into aged hosts improved survival while the opposite effect was observed when they switched the donor/recipient pairs [99]. The same dichotomy was obtained after adoptive transfer of either young or aged Tregs into Treg-depleted mice. They conclude that Tregs lose their pro-repair function with aging, influencing the result of the influenza infection in the lung microenvironment [99].

Lacrimal gland lymphocyte invasion and TLT formation also gradually increase with aging [71, 100], even in individuals with non-immune diseases [70]. Evidence indicates that changes in the type of mucins in the glands of elderly women who receive treatment for dry eyes also occur [72]. Also, TLT in humans have been found in proximity to c-kit + mast cells [101], suggesting that lymphocytes are involved in perpetuating rather than initiating the gland destruction with age [102]. Our results show for the first time that $CD4^+Foxp3^+$ cells are also present in aged human lacrimal glands. We are aimed now at proposing new molecular targets that could potentially delay the immune infiltration in the lacrimal gland with aging. A limitation of our study was the small sample size and a young comparator group. Further studies using a larger sample size are needed to validate our findings. Future studies should focus on further characterizing the kinetics of the different Treg and non-Treg subpopulations that infiltrate the lacrimal gland with aging in different human populations. The better definition of the antigens involved in this process, the TCR repertoire of the lymphocytes and the mediators, either from the innate immune, endocrine, or nervous system, that participate might also help to elucidate potential therapeutic candidates to prolong youth or improve tear film function in the aged ocular surface.

Acknowledgements We gratefully acknowledge Dr. Ron Korstanje, Hannah Donnato, and Laura Robinson from the Nathan Shock Center for Excellence of Aging at Jackson Laboratory for their contribution and Dr. Will Schott at the Flow Cytometry Service at the Jackson Laboratory for the expert assistance with the work described in this publication. We also acknowledge the expert assistance of Brandon Saxton and Joel Sederstrom with the imaging cytometer at Baylor College of Medicine. Leiqi Zhang is acknowledged with the aged colony management. The authors would like to thank Hong Nguyen for the excellent technical assistance (Institute of Functional and Clinical Anatomy, Friedrich-Alexander-Universität Erlangen-Nürnberg). Moreover, the authors sincerely thank those who donated their bodies to science so that anatomical research could be performed.

Author contribution CSdeP and CMT-V were involved in the conception and design of the study. CSdeP, CMT-V, KEM, HH, RGdeS, ZY, JD, and FP were involved in data acquisition. CSdeP, CMT-V, KEM, JGG, JD, and FP were involved in the data analysis and interpretation. CMT-V drafted the manuscript, and CSdeP edited it. All authors contributed to the article and approved the submitted version.

Funding This work was supported by NIH EY030447 (CSdeP), NEI Training Grant in Vision Sciences T32 EY007001 (HH), NIH/NEI EY002520 (Core Grant for Vision Research Department of Ophthalmology), NIH Pathology Core (P30CA125123), BCM Genomic & RNA Profiling Core GARP Core (P30 Digestive Disease Center Support Grant [NIDDK-DK56338]), and Baylor Cytometry and Cell Sorting Core (CPRIT Core Facility Support Award [CPRIT-RP180672], P30 Cancer Center Support Grant [NCI-CA125123], NIH-RR024574, and NIH S10 OD025251 [Union BioMetrica BioSorter]). Further research support was provided by the NIH to the Jackson Laboratory Nathan Shock Center of Excellence in the Basic Biology of Aging (AG038070) Pilot Grant (CSdeP), Research to Prevent Blindness (unrestricted grant to the Department of Ophthalmology), the Hamill Foundation, and the Sid Richardson Foundation and ARVO Roche Collaborative Research Fellowship (JGG). Claudia M. Trujillo-Vargas received supplemental salary support from Facultad de Medicina, Universidad de Antioquia, UdeA, Medellin, Colombia. This work was supported by the Deutsche Forschungsgemeinschaft (DFG) grant PA738/15–1 to FP.

Data availability The original contributions presented in the study are included in the article/Supplementary Material. Further inquiries can be directed to the corresponding author. The datasets for this study can be found in the GEO repository (Access ID GSE192408).

Declarations

Competing interests The authors declare no competing interests.

References

1. Turner VM, Mabbott NA. Ageing adversely affects the migration and function of marginal zone B cells. Immunology. 2017;151(3):349–62.
2. Márquez EJ, Chung CH, Marches R, Rossi RJ, Nehar-Belaid D, Eroglu A, et al. Sexual-dimorphism in human immune system aging. Nat Commun. 2020;11(1):751.
3. Chung HY, Kim DH, Lee EK, Chung KW, Chung S, Lee B, Seo AY, Chung JH, Jung YS, Im E, Lee J, Kim ND, Choi YJ, Im DS, Yu BP. Redefining chronic inflammation in aging and age-related diseases proposal of the senoinflammation concept. Aging Dis. 2019;10(2):367–82.
4. Neyt K, Perros F, GeurtsvanKessel CH, Hammad H, Lambrecht BN. Tertiary lymphoid organs in infection and autoimmunity. Trends Immunol. 2012;33(6):297–305.
5. Ligon MM, Wang C, DeJong EN, Schulz C, Bowdish DME, Mysorekar IU. Single cell and tissue-transcriptomic analysis of murine bladders reveals age- and TNFα-dependent but microbiota-independent tertiary lymphoid tissue formation. Mucosal Immunology. 2020;13(6):908–18.
6. Matossian C, McDonald M, Donaldson KE, Nichols KK, MacIver S, Gupta PK. Dry eye disease: consideration for women's health. Journal of Women's Health (2002) 2019; 28(4):502–514.
7. Williamson J, Gibson AA, Wilson T, Forrester JV, Whaley K, Dick WC. Histology of the lacrimal gland in keratoconjunctivitis sicca. Br J Ophthalmol. 1973;57(11):852–8.
8. de Souza RG, de Paiva CS, Alves MR. Age-related autoimmune changes in lacrimal glands. Immune Network 2019;19(1):e3.
9. de Souza RG, Yu Z, Hernandez H, Trujillo-Vargas CM, Lee A, Mauk KE, et al. Modulation of oxidative stress and inflammation in the aged lacrimal gland. Am J Pathol. 2020;191(2):294–308.
10. Rios JD, Horikawa Y, Chen LL, Kublin CL, Hodges RR, Dartt DA, et al. Age-dependent alterations in mouse exorbital lacrimal gland structure, innervation and secretory response. ExpEye Res. 2005;80(4):477–91.
11. Marinkovic T, Garin A, Yokota Y, Fu Y-X, Ruddle NH, Furtado GC, et al. Interaction of mature CD3+CD4+ T cells with dendritic cells triggers the development of tertiary lymphoid structures in the thyroid. J Clin Investig. 2006;116(10):2622–32.
12. Sharma S, Dominguez AL, Lustgarten J. High accumulation of T regulatory cells prevents the activation of immune responses in aged animals. J Immunol. 2006;177(12):8348–55.
13. Lages CS, Suffia I, Velilla PA, Huang B, Warshaw G, Hildeman DA, et al. Functional regulatory T cells accumulate in aged hosts and promote chronic infectious disease reactivation. J Immunol. 2008;181(3):1835–48.
14. Garg SK, Delaney C, Toubai T, Ghosh A, Reddy P, Banerjee R, et al. Aging is associated with increased regulatory T-cell function. Aging Cell. 2014;13(3):441–8.
15. Chougnet CA, Tripathi P, Lages CS, Raynor J, Sholl A, Fink P, et al. A major role for Bim in regulatory T cell homeostasis. J Immunol. 2011;186(1):156–63.
16. Schmitt V, Rink L, Uciechowski P. The Th17/Treg balance is disturbed during aging. Exp Gerontol. 2013;48(12):1379–86.
17. Derhovanessian E, Chen S, Maier AB, Hähnel K, de Craen AJ, Roelofs H, et al. CCR4+ regulatory T cells accumulate in the very elderly and correlate with superior 8-year survival. J Gerontol A Biol Sci Med Sci. 2015;70(8):917–23.
18. Christodoulou MI, Kapsogeorgou EK, Moutsopoulos NM, Moutsopoulos HM. Foxp3+ T-regulatory cells in Sjogren's syndrome: correlation with the grade of the autoimmune lesion and certain adverse prognostic factors. Am J Pathol. 2008;173(5):1389–96.
19. Sarigul M, Yazisiz V, Bassorgun CI, Ulker M, Avci AB, Erbasan F, et al. The numbers of Foxp3 + Treg cells are positively correlated with higher grade of infiltration at the salivary glands in primary Sjogren's syndrome. Lupus. 2010;19(2):138–45.
20. Coursey TG, Bian F, Zaheer M, Pflugfelder SC, Volpe EA, de Paiva CS. Age-related spontaneous lacrimal keratoconjunctivitis is accompanied by dysfunctional T regulatory cells. Mucosal Immunol. 2017;10(3):743–456.
21. Liston A, Gray DH. Homeostatic control of regulatory T cell diversity. Nat Rev Immunol. 2014;14(3):154–65.
22. Bian F, Xiao Y, Barbosa FL, de Souza RG, Hernandez H, Yu Z, et al. Age-associated antigen-presenting cell alterations promote dry-eye inducing Th1 cells. Mucosal Immunol. 2019;12(4):897–908.
23. Zhang B, Chikuma S, Hori S, Fagarasan S, Honjo T. Nonoverlapping roles of PD-1 and FoxP3 in maintaining immune tolerance in a novel autoimmune pancreatitis mouse model. Proc Natl Acad Sci. 2016;113(30):8490.
24. Liao G, Nayak S, Regueiro JR, Berger SB, Detre C, Romero X, et al. GITR engagement preferentially enhances proliferation of functionally competent CD4+CD25+FoxP3+ regulatory T cells. Int Immunol. 2010;22(4):259–70.
25. Williams-Bey Y, Jiang J, Murasko DM. Expansion of regulatory T cells in aged mice following influenza infection. Mech Ageing Dev. 2011;132(4):163–70.
26. Raynor J, Karns R, Almanan M, Li KP, Divanovic S, Chougnet CA, et al. IL-6 and ICOS antagonize Bim and promote regulatory T cell accrual with age. J Immunol. 2015;195(3):944–52.
27. Mu J, Tai X, Iyer SS, Weissman JD, Singer A, Singer DS. Regulation of MHC class I expression by Foxp3 and its effect on regulatory T cell function. J Immunol. 2014;192(6):2892–903.
28. Walters S, Webster KE, Sutherland A, Gardam S, Groom J, Liuwantara D, et al. Increased $CD4^{+}Foxp3^{+}$ T cells in BAFF-transgenic mice suppress T cell effector responses. J Immunol. 2009;182(2):793.
29. Vences-Catalán F, Rajapaksa R, Srivastava MK, Marabelle A, Kuo CC, Levy R, et al. Tetraspanin CD81, a

modulator of immune suppression in cancer and metastasis. OncoImmunology. 2016;5(5):e1120399.
30. Piconese S, Timperi E, Barnaba V. 'Hardcore' OX40+ immunosuppressive regulatory T cells in hepatic cirrhosis and cancer. OncoImmunology. 2014;3(6):e29257.
31. Lo Re S, Lecocq M, Uwambayinema F, Yakoub Y, Delos M, Demoulin JB, et al. Platelet-derived growth factor-producing CD4+ Foxp3+ regulatory T lymphocytes promote lung fibrosis. Am J Respir Crit Care Med. 2011;184(11):1270–81.
32. Loebbermann J, Thornton H, Durant L, Sparwasser T, Webster KE, Sprent J, et al. Regulatory T cells expressing granzyme B play a critical role in controlling lung inflammation during acute viral infection. Mucosal Immunol. 2012;5(2):161–72.
33. Nishikii H, Kim B-S, Yokoyama Y, Chen Y, Baker J, Pierini A, et al. DR3 signaling modulates the function of Foxp3+ regulatory T cells and the severity of acute graft-versus-host disease. Blood. 2016;128(24):2846–58.
34. Panduro M, Benoist C, Mathis D. Tissue Tregs. Annu Rev Immunol. 2016;34(1):609–33.
35. Deane JA, Abeynaike LD, Norman MU, Wee JL, Kitching AR, Kubes P, et al. Endogenous regulatory T cells adhere in inflamed dermal vessels via ICAM-1: association with regulation of effector leukocyte adhesion. J Immunol. 2012;188(5):2179.
36. Wheaton JD, Yeh CH, Ciofani M. Cutting edge: c-Maf is required for regulatory T cells to adopt RORγt(+) and follicular phenotypes. J Immunol. 2017;199(12):3931–6.
37. Liu T, Soong L, Liu G, König R, Chopra AK. CD44 expression positively correlates with Foxp3 expression and suppressive function of CD4+ Treg cells. Biol Direct. 2009;4(1):40.
38. Rappl G, Schmidt A, Mauch C, Hombach AA, Abken H. Extensive amplification of human regulatory T cells alters their functional capacities and targets them to the periphery. Rejuvenation Res. 2008;11(5):915–33.
39. Chauhan SK, El AJ, Ecoiffier T, Goyal S, Zhang Q, Saban DR, et al. Autoimmunity in dry eye is due to resistance of Th17 to Treg suppression. J Immunol. 2009;182(3):1247–52.
40. de Paiva CS, Villarreal AL, Corrales RM, Rahman HT, Chang VY, Farley WJ, et al. Dry eye-induced conjunctival epithelial squamous metaplasia is modulated by interferon-gamma. Invest Ophthalmol Vis Sci. 2007;48(6):2553–60.
41. Schaumburg CS, Siemasko KF, de Paiva CS, Wheeler LA, Niederkorn JY, Pflugfelder SC, et al. Ocular surface APCs are necessary for autoreactive T cell-mediated experimental autoimmune lacrimal keratoconjunctivitis. J Immunol. 2011;187(7):3653–62.
42. Kitz A, Dominguez-Villar M. Molecular mechanisms underlying Th1-like Treg generation and function. Cell Mol Life Sci. 2017;74(22):4059–75.
43. Koch MA, Thomas KR, Perdue NR, Smigiel KS, Srivastava S, Campbell DJ. T-bet(+) Treg cells undergo abortive Th1 cell differentiation due to impaired expression of IL-12 receptor β2. Immunity. 2012;37(3):501–10.
44. Koch MA, Tucker-Heard G, Perdue NR, Killebrew JR, Urdahl KB, Campbell DJ. The transcription factor T-bet controls regulatory T cell homeostasis and function during type 1 inflammation. Nat Immunol. 2009;10(6):595–602.
45. Oldenhove G, Bouladoux N, Wohlfert EA, Hall JA, Chou D, Dos Santos L, et al. Decrease of Foxp3+ Treg cell number and acquisition of effector cell phenotype during lethal infection. Immunity. 2009;31(5):772–86.
46. Zhao J, Zhao J, Fett C, Trandem K, Fleming E, Perlman S. IFN-γ- and IL-10-expressing virus epitope-specific Foxp3(+) T reg cells in the central nervous system during encephalomyelitis. J Exp Med. 2011;208(8):1571–7.
47. Turner VM, Mabbott NA. Structural and functional changes to lymph nodes in ageing mice. Immunol. 2017;151(2):239–47.
48. Goronzy JJ, Weyand CM. Mechanisms underlying T cell ageing. Nat Rev Immunol. 2019;19(9):573–83.
49. Honey K. CCL3 and CCL4 actively recruit CD8+ T cells. Nat Rev Immunol. 2006;6(6):427–427.
50. Dock J, Ramirez CM, Hultin L, Hausner MA, Hultin P, Elliott J, et al. Distinct aging profiles of CD8+ T cells in blood versus gastrointestinal mucosal compartments. PLoS One. 2017;12(8):e0182498.
51. Francis JN, Sabroe I, Lloyd CM, Durham SR, Till SJ. Elevated CCR6+ CD4+ T lymphocytes in tissue compared with blood and induction of CCL20 during the asthmatic late response. Clin Exp Immunol. 2008;152(3):440–7.
52. Podojil JR, Kohm AP, Miller SD. CD4+ T cell expressed CD80 regulates central nervous system effector function and survival during experimental autoimmune encephalomyelitis. J Immunol. 2006;177(5):2948–58.
53. Farr L, Ghosh S, Jiang N, Watanabe K, Parlak M, Bucala R, et al. CD74 signaling links inflammation to intestinal epithelial cell regeneration and promotes mucosal healing. Cell Mol Gastroenterol Hepatol. 2020;10(1):101–12.
54. Channappanavar R, Twardy BS, Krishna P, Suvas S. Advancing age leads to predominance of inhibitory receptor expressing CD4 T cells. Mech Ageing Dev. 2009;130(10):709–12.
55. Ehrlich AK, Pennington JM, Tilton S, Wang X, Marshall NB, Rohlman D, et al. AhR activation increases IL-2 production by alloreactive CD4+ T cells initiating the differentiation of mucosal-homing Tim3+Lag3+ Tr1 cells. Eur J Immunol. 2017;47(11):1989–2001.
56. Hiramatsu Y, Suto A, Kashiwakuma D, Kanari H, Kagami S-I, Ikeda K, et al. c-Maf activates the promoter and enhancer of the IL-21 gene, and TGF-β inhibits c-Maf-induced IL-21 production in CD4+ T cells. J Leukoc Biol. 2010;87(4):703–12.
57. Fu S-H, Yeh L-T, Chu C-C, Yen BL-J, Sytwu H-K. New insights into Blimp-1 in T lymphocytes a divergent regulator of cell destiny and effector function. J Biomed Sci. 2017;24(1):49.
58. Tau GZ, von der Weid T, Lu B, Cowan S, Kvatyuk M, Pernis A, et al. Interferon gamma signaling alters the function of T helper type 1 cells. J Exp Med. 2000;192(7):977–86.
59. Bishu S, Hernández-Santos N, Simpson-Abelson MR, Huppler AR, Conti HR, Ghilardi N, et al. The adaptor CARD9 is required for adaptive but not innate

immunity to oral mucosal Candida albicans infections. Infect Immun. 2014;82(3):1173–80.
60. De Fanis U, Wang GC, Fedarko NS, Walston JD, Casolaro V, Leng SX. T-Lymphocytes expressing CC chemokine receptor-5 are increased in frail older adults. J Am Geriatr Soc. 2008;56(5):904–8.
61. Wherry EJ, Kurachi M. Molecular and cellular insights into T cell exhaustion. Nat Rev Immunol. 2015;15(8):486–99.
62. Mueller A, Strange PG. CCL3, acting via the chemokine receptor CCR5, leads to independent activation of Janus kinase 2 (JAK2) and Gi proteins. FEBS Lett. 2004;570(1–3):126–32.
63. Paley MA, Kroy DC, Odorizzi PM, Johnnidis JB, Dolfi DV, Barnett BE, et al. Progenitor and terminal subsets of CD8+ T cells cooperate to contain chronic viral infection. Science. 2012;338(6111):1220–5.
64. López-Yglesias AH, Burger E, Araujo A, Martin AT, Yarovinsky F. T-bet-independent Th1 response induces intestinal immunopathology during Toxoplasma gondii infection. Mucosal Immunol. 2018;11(3):921–31.
65. Harpaz I, Bhattacharya U, Elyahu Y, Strominger I, Monsonego A. Old mice accumulate activated effector CD4 T cells refractory to regulatory T cell-induced immunosuppression. Front Immunol. 2017;8:283.
66. Klann JE, Kim SH, Remedios KA, He Z, Metz PJ, Lopez J, et al. Integrin activation controls tegulatory T cell–mediated peripheral tolerance. J Immunol. 2018;200(12):4012.
67. Lei Y, Takahama Y. XCL1 and XCR1 in the immune system. Microbes Infect. 2012;14(3):262–7.
68. Mattoo H, Mahajan VS, Maehara T, Deshpande V, Della-Torre E, Wallace ZS, et al. Clonal expansion of CD4(+) cytotoxic T lymphocytes in patients with IgG4-related disease. J Allergy Clin Immunol. 2016;138(3):825–38.
69. Hughes-Fulford M, Sugano E, Schopper T, Li C-F, Boonyaratanakornkit JB, Cogoli A. Early immune response and regulation of IL-2 receptor subunits. Cell Signal. 2005;17(9):1111–24.
70. Nasu M, Matsubara O, Yamamoto H. Post-mortem prevalence of lymphocytic infiltration of the lacrymal gland: a comparative study in autoimmune and non-autoimmune diseases. J Pathol. 1984;143(1):11–5.
71. Damato BE, Allan D, Murray SB, Lee WR. Senile atrophy of the human lacrimal gland: the contribution of chronic inflammatory disease. Br J Ophthalmol. 1984;68(9):674–80.
72. Paulsen F, Langer G, Hoffmann W, Berry M. Human lacrimal gland mucins. Cell Tissue Res. 2004;316(2):167–77.
73. Obata H. Anatomy and histopathology of the human lacrimal gland. Cornea. 2006;25(10 Suppl 1):S82–9.
74. Gudmundsson OG, Benediktsson H, Olafsdottir K. T-lymphocyte subsets in the human lacrimal gland. Acta Ophthalmol. 1988;66(1):19–23.
75. Gudmundsson OG, Bjornsson J, Olafsdottir K, Bloch KJ, Allansmith MR, Sullivan DA. T cell populations in the lacrimal gland during aging. Acta Ophthalmol. 1988;66(5):490–7.
76. Wieczorek R, Jakobiec FA, Sacks EH, Knowles DM. The immunoarchitecture of the normal human lacrimal gland Relevancy for understanding pathologic conditions. Ophthalmol. 1988;95(1):100–9.
77. Segerberg-Konttinen M. Focal adenitis in lacrimal and salivary glands A post-mortem study. Scand J Rheumatol. 1988;17(5):379–85.
78. Volpe EA, Henriksson JT, Wang C, Barbosa FL, Zaheer M, Zhang X, et al. Interferon-gamma deficiency protects against aging-related goblet cell loss. Oncotarget. 2016;7(40):64605–6461.
79. Perkins JR, Dawes JM, McMahon SB, Bennett DL, Orengo C, Kohl M. ReadqPCR and NormqPCR: R packages for the reading, quality checking and normalisation of RT-qPCR quantification cycle (Cq) data. BMC Genomics. 2012;13:296.
80. Hennig C. Cran-package fpc. https://cran.r-project.org/web/packages/fpc/index.html. Accessed Jan 2021.
81. Alexa A, J. R. topGO: enrichment analysis for Gene Ontology. R package version 1381, 2019.
82. Mitchell AL, Attwood TK, Babbitt PC, Blum M, Bork P, Bridge A, et al. InterPro in 2019: improving coverage, classification and access to protein sequence annotations. Nucleic Acids Res. 2019;47(D1):D351-d360.
83. Geer LY, Marchler-Bauer A, Geer RC, Han L, He J, He S, et al. The NCBI BioSystems database. Nucleic Acids Res. 2010;38(Database issue):D492-496.
84. Subramanian A, Tamayo P, Mootha VK, Mukherjee S, Ebert BL, Gillette MA, et al. Gene set enrichment analysis: a knowledge-based approach for interpreting genome-wide expression profiles. Proc Natl Acad Sci USA. 2005;102(43):15545–50.
85. Liberzon A, Subramanian A, Pinchback R, Thorvaldsdóttir H, Tamayo P, Mesirov JP. Molecular signatures database (MSigDB) 3.0. Bioinforma. 2011;27(12):1739–40.
86. Fabregat A, Jupe S, Matthews L, Sidiropoulos K, Gillespie M, Garapati P, et al. The Reactome Pathway Knowledgebase. Nucleic Acids Res. 2018;46(D1):D649-d655.
87. Slenter DN, Kutmon M, Hanspers K, Riutta A, Windsor J, Nunes N, et al. WikiPathways: a multifaceted pathway database bridging metabolomics to other omics research. Nucleic Acids Res. 2018;46(D1):D661-d667.
88. Oliveros JC. Venny. An interactive tool for comparing lists with Venn's diagrams. 2017. https://bioinfogp.cnb.csic.es/tools/venny/indexhtml. Accessed Jan 2021.
89. Elyahu Y, Hekselman I, Eizenberg-Magar I, Berner O, Strominger I, Schiller M, et al. Aging promotes reorganization of the CD4 T cell landscape toward extreme regulatory and effector phenotypes. Sci Adv. 2019;5(8):eaaw8330.
90. Appay V, Sauce D. Naive T cells: the crux of cellular immune aging? Exp Gerontol. 2014;54:90–3.
91. Min B. Spontaneous T cell proliferation: a physiologic process to create and maintain homeostatic balance and diversity of the immune system. Frontiers in Immunology. 2018;19(9):547.
92. Koch S, Larbi A, Özcelik D, Solana R, Gouttefangeas C, Attig S, et al. Cytomegalovirus infection. Annals New York Acad Sci. 2007;1114(1):2335.

93. Pflugfelder SC, Crouse CA, Monroy D, Yen M, Rowe M, Atherton SS. Epstein-Barr virus and the lacrimal gland pathology of Sjogren's syndrome. Am J Pathol. 1993;143(1):49–64.
94. Soon MSF, Engel JA, Lee HJ, Haque A. Development of circulating CD4+ T-cell memory. Immunol Cell Biol. 2019;97(7):617–24.
95. Fang F, Yu M, Cavanagh Mary M, Hutter Saunders J, Qi Q, Ye Z, et al. Expression of CD39 on activated T cells impairs their survival in older individuals. Cell Rep. 2016;14(5):1218–31.
96. Guerrini Matteo M, Okamoto K, Komatsu N, Sawa S, Danks L, Penninger Josef M, et al. Inhibition of the TNF family cytokine RANKL prevents autoimmune inflammation in the central nervous system. Immunity. 2015;43(6):1174–85.
97. Akimova T, Levine MH, Beier UH, Hancock WW. Standardization, evaluation, and area-under-curve analysis of human and murine Treg suppressive function. Methods in Mol Biol (Clifton, NJ). 2016;1371:43–78.
98. Nishioka T, Shimizu J, Iida R, Yamazaki S, Sakaguchi S. CD4+CD25+Foxp3+ T cells and CD4+CD25-Foxp3+ T cells in aged mice. J Immunol. 2006;176(11):6586–93.
99. Morales-Nebreda L, Helmin KA, Torres Acosta MA, Markov NS, Hu JY, Joudi AM et al. Aging imparts cell-autonomous dysfunction to regulatory T cells during recovery from influenza pneumonia. JCI Insight 2021;6(6):e141690.
100. Obata H, Yamamoto S, Horiuchi H, Machinami R. Histopathologic study of human lacrimal gland. Statistical analysis with special reference to aging. Ophthalmol. 1995;102(4):678–86.
101. Perros F, Dorfmüller P, Montani D, Hammad H, Waelput W, Girerd B, et al. Pulmonary lymphoid neogenesis in idiopathic pulmonary arterial hypertension. Am J Respir Crit Care Med. 2012;185(3):311–21.
102. Rocha EM, Alves M, Rios JD, Dartt DA. The aging lacrimal gland: changes in structure and function. Ocul Surf. 2008;6(4):162–74.